

Chapter 2

Linear Propagation

In this chapter we consider the propagation of continuous-wave (cw) laser beams in a linear medium.¹

2.1 Geometrical Optics

Laser beams that propagate in a Kerr medium can become narrower with propagation, a phenomenon called *self focusing*. The simplest and most intuitive way to understand why a Kerr nonlinearity leads to self focusing is to use *geometrical optics* (Sect. 3.2).² Therefore, we begin by introducing the geometrical optics approximation.

Our starting point is the dimensional linear Helmholtz equation

$$\Delta E(\mathbf{x}) + k^2 \left(\frac{\mathbf{x}}{X} \right) E = 0, \quad k^2 \left(\frac{\mathbf{x}}{X} \right) = \frac{\omega_0^2}{c^2} n^2 \left(\frac{\mathbf{x}}{X} \right), \quad (2.1)$$

which models propagation in an inhomogeneous linear medium. Here, $\mathbf{x} = (x, y, z)$, n is the linear index of refraction,³ and X is the characteristic length-scale for changes in n (hence in k). We assume that the medium is weakly inhomogeneous, i.e., $k \approx k_0 = \omega_0 n_0 / c$.⁴ Let $\lambda = 2\pi / k_0$ be the wavelength. The geometrical optics approximation is valid when $X \gg \lambda$, i.e., when changes in n occur over distances much longer than the wavelength, so that locally (i.e., over a few wavelengths) the material can be viewed as homogeneous.

¹ Since all media are nonlinear (Sect. 1.4.2), the term *linear medium* refers to the situation where the electric field is sufficiently weak, see (1.37), so that nonlinear effects are negligible.

² Indeed, the early studies on self-focusing employed a geometrical optics approach (Sects. 3.2 and 3.3.2).

³ To simplify the notations, in this chapter (only) we denote the inhomogeneous linear index of refraction by $n(\cdot)$, and its value in the absence of inhomogeneities by n_0 .

⁴ This is the linear analog of a weakly-nonlinear homogeneous Kerr medium, i.e., when the contribution of the nonlinear Kerr effect to the index of refraction is small, see (1.29).

Let us change to the dimensionless variables

$$\tilde{\mathbf{x}} = \frac{\mathbf{x}}{X}, \quad \tilde{E} = \frac{E}{E_c},$$

where E_c is the characteristic magnitude of E . Then the dimensionless Helmholtz equation reads

$$\Delta_{\tilde{\mathbf{x}}} \tilde{E}(\tilde{\mathbf{x}}) + \tilde{k}^2(\tilde{\mathbf{x}}) \tilde{E} = 0,$$

where $\tilde{k} = Xk$ is the dimensionless wavenumber. Since $X \gg \lambda$,

$$\tilde{k} \approx \tilde{k}_0 := Xk_0 = \frac{2\pi X}{\lambda} \gg 1.$$

To simplify the notations, from now on we drop the tildes. Thus, the dimensionless Helmholtz equation reads

$$\Delta E(\mathbf{x}) + k^2(\mathbf{x}) E = 0, \quad (2.2)$$

and the dimensionless geometrical optics regime is $k^2 \gg 1$.

2.1.1 Eikonal Equation

When $k \approx k_0 \gg 1$, we can look for solutions of (2.2) of the form⁵

$$E = A(\mathbf{x}) e^{ik_0 S(\mathbf{x})},$$

where A and S are real. Here, A is the *slowly-varying envelope* and $k_0 S$ is the *phase*. Substitution in (2.2) gives

$$\Delta A + 2ik_0 \nabla A \cdot \nabla S + A(ik_0 \Delta S - k_0^2 \nabla S \cdot \nabla S) + k^2 A = 0, \quad (2.3)$$

where $\nabla = \left(\frac{\partial}{\partial x}, \frac{\partial}{\partial y}, \frac{\partial}{\partial z} \right)$. Balancing the leading $O(k_0^2)$ terms in (2.3) gives the *eikonal equation*

$$\nabla S \cdot \nabla S = \tilde{n}^2(\mathbf{x}), \quad (2.4)$$

where

$$\tilde{n}(\mathbf{x}) = \frac{k(\mathbf{x})}{k_0} = \frac{n(\mathbf{x})}{n_0} \approx 1.$$

The initial condition for the eikonal equation is $S(\mathbf{x}) = S_0(\mathbf{x})$ for $\mathbf{x} \in \Sigma_0$, where Σ_0 is a given surface in \mathbb{R}^3 . For example, the model problem studied in this

⁵ This ansatz can be viewed as a generalization of the plane-wave solution (1.12).

book is the propagation of a laser beam in the half-space $z > 0$, given an incoming beam $E_0^{\text{inc}}(x, y)$ at $z = 0$ (Fig. 1.1). In this case, Σ_0 is the (x, y) -plane $z \equiv 0$.

The eikonal equation is a nonlinear first-order PDE. As such, it can be solved using the *method of characteristics*.^{6,7} To do that, let us recall the method of characteristics for the first-order linear PDE

$$a(\mathbf{x})u_x(\mathbf{x}) + b(\mathbf{x})u_y + c(\mathbf{x})u_z = e(\mathbf{x}). \quad (2.5)$$

The characteristic curves $\mathbf{x}(\sigma) = (x(\sigma), y(\sigma), z(\sigma))$ of (2.5), where σ is the curve parameter, are parallel to (a, b, c) . Therefore,

$$\frac{d\mathbf{x}(\sigma)}{d\sigma} = \eta(\sigma) (a(\mathbf{x}(\sigma)), b(\mathbf{x}(\sigma)), c(\mathbf{x}(\sigma))), \quad (2.6a)$$

where $\eta(\sigma)$ is an arbitrary positive function. By the chain rule, the evolution of u along characteristics is

$$\frac{du(\mathbf{x}(\sigma))}{d\sigma} = \nabla u \cdot \frac{d\mathbf{x}}{d\sigma} = \eta(\sigma) e(\mathbf{x}(\sigma)). \quad (2.6b)$$

Therefore, to solve the PDE (2.5), one only needs to solve the ODEs (2.6).

Unlike (2.5), the eikonal equation (2.4) is nonlinear. Nevertheless, since the vector ∇S in (2.4) “corresponds” to the vector (a, b, c) in (2.5), this suggests that the characteristics of the eikonal equation are parallel to ∇S , i.e.,

$$\frac{d\mathbf{x}}{d\sigma} = \eta(\sigma) \nabla S.$$

Let σ be the arclength. Then

$$1 = \left| \frac{d\mathbf{x}}{d\sigma} \right|^2 = \eta^2 (\nabla S)^2 = \eta^2 \tilde{n}^2.$$

Hence, $\eta = 1/\tilde{n}$ and

$$\frac{d\mathbf{x}}{d\sigma} = \frac{1}{\tilde{n}} \nabla S. \quad (2.7)$$

To close the system (2.7), we note that

$$\begin{aligned} \frac{d}{d\sigma} \nabla S(\mathbf{x}(\sigma)) &= \nabla(\nabla S) \cdot \frac{d\mathbf{x}}{d\sigma} = \nabla(\nabla S) \cdot \frac{1}{\tilde{n}} \nabla S = \frac{1}{2\tilde{n}} \nabla(\nabla S)^2 \\ &= \frac{1}{2\tilde{n}} \nabla(\tilde{n}^2) = \nabla \tilde{n}. \end{aligned}$$

⁶ See e.g., [210].

⁷ In geometrical optics the characteristics are also called *rays*, because they correspond to the curves followed by light rays.

Therefore, the rays of the eikonal equation are determined by the system of six linear ODEs

$$\frac{d\mathbf{x}}{d\sigma} = \frac{1}{\tilde{n}}\mathbf{p}, \quad \frac{d\mathbf{p}}{d\sigma} = \nabla\tilde{n}, \quad (2.8)$$

where $\mathbf{p} = \nabla S$ and $\tilde{n} = n/n_0$.

Definition 2.1 (wavefront) *In optics, a surface of points that have the same phase is called a wavefront.*

Since ∇S is perpendicular to the wavefronts, we have

Lemma 2.1 *Under the geometrical optics approximation, the rays of the eikonal equation are perpendicular to the wavefronts of the Helmholtz solution.*

The evolution of S along a ray is given by

$$\frac{d}{d\sigma}S(\mathbf{x}(\sigma)) = \nabla S \cdot \frac{d\mathbf{x}}{d\sigma} = \frac{1}{\tilde{n}}(\nabla S)^2 = \tilde{n}. \quad (2.9)$$

Therefore,

$$dS = \tilde{n}d\sigma = \frac{n}{n_0}d\sigma = \frac{c/n_0}{c/n}d\sigma = \frac{c}{n_0} \frac{d\sigma}{v},$$

where $v(\mathbf{x}) = c/n(\mathbf{x})$ is the local speed of propagation. Since $d\sigma/v = dt$, then

$$dS = \frac{c}{n_0}dt. \quad (2.10)$$

Therefore, $S(\mathbf{x}(\sigma))$ measures the *travel time* along the ray.

Fermat's principle of least time states that out of all possible paths from one point to another, a light ray travels along the path with the shortest travel-time. It later turned out that a more accurate formulation is the *principle of stationary time*, which states that out of all possible paths from point \mathbf{x}_0 to point \mathbf{x}_1 , a light ray travels along the path whose travel-time is stationary with respect to neighboring paths that connect \mathbf{x}_0 and \mathbf{x}_1 . In other words, the ray that connects \mathbf{x}_0 and \mathbf{x}_1 is an extremal of the functional

$$T = \int_{\text{path } \mathbf{x}_0 \rightarrow \mathbf{x}_1} \frac{d\sigma}{v(\mathbf{x}(\sigma))}. \quad (2.11)$$

Exercise 2.1 *Show that the trajectories of the rays, as given by Eq. (2.8), are indeed the extremals of the functional (2.11).*

1. Write the functional using a parameter μ with fixed boundary values

$$T = \frac{1}{c} \int_{\mu=0}^1 \mathcal{F}(x(\mu), y(\mu), z(\mu), x_\mu, y_\mu, z_\mu) d\mu,$$

where $\mathcal{F} = n(x, y, z)\sqrt{(x_\mu)^2 + (y_\mu)^2 + (z_\mu)^2}$.

2. Write the Euler-Lagrange equations for an extremal

$$\mathcal{F}_x - \frac{d}{d\mu} \mathcal{F}_{x_\mu} = 0, \quad \mathcal{F}_y - \frac{d}{d\mu} \mathcal{F}_{y_\mu} = 0, \quad \mathcal{F}_z - \frac{d}{d\mu} \mathcal{F}_{z_\mu} = 0.$$

3. Change back from μ to σ .

Fermat's principle is not an exact physical law. Rather, it is an approximate physical law, which is valid under the geometrical optics approximation. This is not really surprising, since it is based on a ray description of light propagation.

Lemma 2.2 *Rays follow the same path in both directions.*

Proof This follows from the fact that the characteristic equations (2.8) remain unchanged under the *reversibility transformation* $\sigma \rightarrow -\sigma$ and $S \rightarrow -S$. Alternatively, it follows directly from Fermat's principle. \square

Remark Since S increases in the direction of propagation of the ray, see (2.10), S changes to $-S$ when we reverse the direction of propagation.

2.1.2 Transport Equation

The balance of the $O(k_0)$ terms in (2.3) gives the *transport equation*

$$2\nabla S \cdot \nabla A + A\Delta S = 0. \quad (2.12)$$

Since S has already been determined by the eikonal equation, (2.12) is a first-order linear PDE for A . By (2.6), the characteristics of this equation are parallel to ∇S . Therefore, they identify with the rays of S . The change in A along a ray is

$$\frac{d}{d\sigma} A(\mathbf{x}(\sigma)) = \nabla A \cdot \frac{d\mathbf{x}}{d\sigma} = \frac{1}{\tilde{n}} \nabla A \cdot \nabla S = -\frac{1}{2\tilde{n}} A\Delta S,$$

where $\mathbf{x}(\sigma)$ and $S = S(\mathbf{x}(\sigma))$ were already calculated from (2.8) and (2.9), respectively, and $\tilde{n} = \tilde{n}(\mathbf{x}(\sigma))$ is given. Therefore, $A(\mathbf{x}(\sigma))$ is calculated from the ODE

$$\frac{1}{A} \frac{dA}{d\sigma} = -\frac{1}{2\tilde{n}} \Delta S.$$

The transport equation can be written as

$$A^2 \Delta S + \nabla \left(A^2 \right) \cdot \nabla S = 0, \quad (2.13)$$

or, in divergence form, as

$$\nabla \cdot (A^2 \nabla S) = 0.$$

To understand the conservation law associated with this equation, consider a *bundle (tube) of rays* that start from a surface Σ_0 , and denote by Σ_1 the surface defined by the positions of the rays at $\sigma = \sigma_1$.⁸ These rays form a tube with ends Σ_0 and Σ_1 and sides Σ_{sides} . By the divergence theorem,

$$0 = \int_{\substack{\text{tube} \\ \text{volume}}} \nabla \cdot (A^2 \nabla S) \, d\mathbf{x} = \int_{\substack{\text{tube} \\ \text{surface}}} A^2 \nabla S \cdot \mathbf{n} \, ds,$$

where \mathbf{n} is the outward normal to the ray bundle,⁹ and ds is a surface element. Since the rays are parallel to ∇S ,

$$\nabla S \cdot \mathbf{n} = \begin{cases} 0, & \text{on } \Sigma_{\text{sides}}, \\ -|\nabla S|, & \text{on } \Sigma_0, \\ |\nabla S|, & \text{on } \Sigma_1. \end{cases}$$

Combining the above and using (2.4) and $\tilde{n}(\mathbf{x}) = n(\mathbf{x})/n_0$ gives

$$\int_{\Sigma_0} n A^2 \, ds = \int_{\Sigma_1} n A^2 \, ds. \quad (2.14)$$

In optics $\int_{\Sigma} n |A|^2 \, ds$ is the *beam power* at Σ . Hence, the transport equation leads to

Lemma 2.3 *Under the geometrical optics approximation, the power of a ray bundle at any cross-section $\sigma \equiv \text{constant}$ is constant.*

Relation (2.14) shows that when an input beam is focused by a lens, all the beam power concentrates at the focal point:¹⁰

Corollary 2.1 *Consider a focused input beam that propagates in a homogeneous medium. Then under the geometrical optics approximation*

$$n |A|^2 \rightarrow P \cdot \delta(\mathbf{x} - \mathbf{x}_c), \quad \mathbf{x} \rightarrow \mathbf{x}_c,$$

where P is the input power, $\mathbf{x}_c \in \mathbb{R}^3$ is the focal point of the lens, and the limit is in the sense of distributions. In particular, $A(\mathbf{x})$ becomes infinite as $\mathbf{x} \rightarrow \mathbf{x}_c$.

Proof Let the input beam be prescribed at Σ_0 . Then its power is $P = \int_{\Sigma_0} n A^2$. Since all the rays reach the focal point with the same σ (see Exercise 2.5 below), the result follows from relation (2.14) with $\Sigma_1 = \mathbf{x}_c$. \square

⁸ I.e., $\Sigma_1 = \{\mathbf{x}(\sigma_1) \mid \mathbf{x}(0) \in \Sigma_0\}$.

⁹ Not to be confused with n , the index of refraction.

¹⁰ This property is called *whole-beam collapse* (Sect. 7.7).

Remark Let S and A be the solutions of the eikonal equation (2.4) and the transport equation (2.12), respectively. Then $E_{\text{go}} := Ae^{ik_0 S}$ is only an approximate solution of the Helmholtz equation (2.2), since we neglected the diffraction term ΔA in (2.3).

2.2 Applications of Geometrical Optics

2.2.1 Homogeneous Medium

When $n \equiv n_0$, Fermat's principle of "least time" is the same as the principle of "least distance", showing that rays move in straight lines. This also follows from Eq. (2.8), which in a homogeneous medium ($\tilde{n} \equiv 1$) read

$$\frac{d\mathbf{x}}{d\sigma} = \mathbf{p}, \quad \frac{d\mathbf{p}}{d\sigma} = 0.$$

2.2.2 Snell's Law

Consider a two-layer medium that consists of material 1 with linear refractive index $n(x, y, z) \equiv n_1$ at $y > 0$, and material 2 with $n(x, y, z) \equiv n_2$ at $y < 0$. Now, consider a ray which travels from point $\mathbf{A} = (x_1, y_1, z_1)$ inside material 1 to point $\mathbf{B} = (x_2, y_2, z_2)$ inside material 2, and crosses the interface $y = 0$ at point $\mathbf{C} = (x, 0, z)$, see Fig. 2.1. Within each material the ray travels in a straight line, i.e., $\overline{\mathbf{AC}}$ and $\overline{\mathbf{CB}}$ are straight lines. Since the propagation velocity in material i is c/n_i , the overall travel-time from \mathbf{A} to \mathbf{C} to \mathbf{B} is

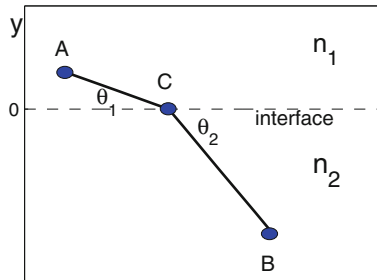


Fig. 2.1 Derivation of Snell's law

$$T = \frac{n_1}{c} \overline{AC} + \frac{n_2}{c} \overline{CB} = \sum_{i=1}^2 \frac{n_i}{c} \sqrt{(x - x_i)^2 + y_i^2 + (z - z_i)^2}.$$

Exercise 2.2 Use Fermat's principle of least time to show that

$$n_1 \cos \theta_1 = n_2 \cos \theta_2, \quad (\text{Snell's law}) \quad (2.15)$$

where θ_i is the angle that a ray inside material i makes with the interface (see Fig. 2.1).¹¹

Remark From Snell's law we see that

$$n_2 > n_1 \implies \cos \theta_2 < \cos \theta_1 \implies \theta_2 > \theta_1,$$

i.e., rays bend towards regions with a higher index of refraction.

Remark Snell's law explains why a teaspoon which is partially immersed in a cup of tea appears to be bent (and also why n is called the *index of refraction*).

Exercise 2.3 Show that if a ray is reflected back by a planar mirror, the angle of incidence is equal to the angle of reflection.

2.2.3 Linear Waveguides

Two Layers

Consider a *planar waveguide* made out of an inner core with index of refraction n_1 at $0 \leq |y| < y_1$, and an outer cladding with index of refraction n_2 at $y_1 < |y| < y_2$. Inside each dielectric the rays travel in straight lines. Let us denote by θ_1 the angle at which an inner-core ray impinges on the interface with the outer cladding at $y = \pm y_1$, and by θ_2 the angle at which the ray enters the outer cladding. By Snell's law,

$$n_1 \cos \theta_1 = n_2 \cos \theta_2.$$

Therefore, θ_2 can be found from the equation

$$\cos \theta_2 = \frac{n_1}{n_2} \cos \theta_1. \quad (2.16)$$

If $n_1 < n_2$, Eq. (2.16) can always be solved for θ_2 , since for any θ_1 the magnitude of the right-hand side of (2.16) is less than one. Physically, this means that rays can always cross the interface. If $n_1 > n_2$, however, then for all the inner-core rays for which

¹¹ Here the angle is defined with respect to the interface, hence the use of cosines instead of sines.

$$|\theta_1| < \Theta_{\text{cr}} := \cos^{-1} \left(\frac{n_2}{n_1} \right), \quad (2.17)$$

the right-hand side of (2.16) is larger than one, and so we cannot solve for θ_2 . Physically, this means that these rays cannot cross the interface. Instead, they are reflected backwards into the inner core. We thus see that when $n_1 > n_2$, the planar waveguide traps the paraxial rays $|\theta_1| \leq \Theta_{\text{cr}}$ inside the inner core, and that the *trapping efficiency* increases with the ratio n_1/n_2 .

K Layers

Let us consider now a planar waveguide made out of K dielectric materials, such that the index of refraction is n_k for $y_{k-1} < |y| < y_k$, where $k = 1, \dots, K$, and $y_0 = 0$. Since at each interface

$$n_k \cos \theta_k = n_{k+1} \cos \theta_{k+1}, \quad k = 1, \dots, K-1,$$

and since between interfaces rays travel in straight lines, it follows that for any given ray,

$$n_1 \cos \theta_1 = n_2 \cos \theta_2 = \dots = n_K \cos \theta_K. \quad (2.18)$$

Therefore, if n_k is monotonically decreasing in k , then so does θ_k , i.e., at each interface the ray bends back towards the center ($y = 0$). In addition, relation (2.18) shows that the overall trapping efficiency depends on n_1/n_K .

Continuous Variation

Consider now a planar waveguide made out of a dielectric material with a continuously-varying index of refraction $n = n(y)$. Intuitively, we can think of this waveguide as the limit as $K \rightarrow \infty$ of a planar waveguide with K homogeneous layers. Taking the limit of (2.18) as $K \rightarrow \infty$ shows that the trajectory of the ray satisfies

$$n(y) \cos \theta(y) \equiv n(0) \cos \theta(0). \quad (2.19)$$

We can also derive (2.19) from the eikonal equation. Indeed, when $n = n(y)$, Eqs. (2.8) for the trajectories of the rays read

$$\begin{aligned} \frac{dx}{d\sigma} &= \frac{p_1}{\tilde{n}}, & \frac{dy}{d\sigma} &= \frac{p_2}{\tilde{n}}, & \frac{dz}{d\sigma} &= \frac{p_3}{\tilde{n}}, \\ \frac{dp_1}{d\sigma} &= 0, & \frac{dp_2}{d\sigma} &= \frac{d\tilde{n}}{dy}, & \frac{dp_3}{d\sigma} &= 0. \end{aligned}$$

Therefore, p_1 and p_3 are constants. Let $\theta(\sigma)$ denote the angle at $\mathbf{x}(\sigma)$ between the ray and its projection on the (x, z) -plane $y \equiv y(\sigma)$. Then, since $|\frac{d\mathbf{x}}{d\sigma}| = 1$,

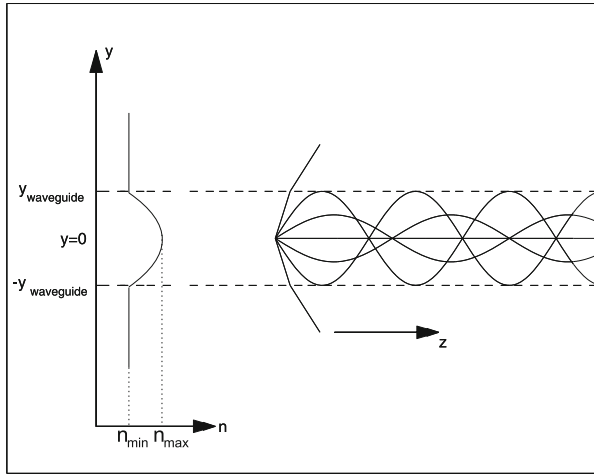


Fig. 2.2 Propagation of rays in a planar waveguide with a continuously-varying index of refraction $n = n(y)$

$$\cos \theta = \frac{\sqrt{\left(\frac{dx}{d\sigma}\right)^2 + \left(\frac{dz}{d\sigma}\right)^2}}{\left|\frac{dx}{d\sigma}\right|} = \sqrt{\frac{p_1^2(0)}{\tilde{n}^2(y)} + \frac{p_3^2(0)}{\tilde{n}^2(y)}}.$$

Hence, $n(y) \cos \theta \equiv \text{constant}$, which is (2.19).

Let us assume that $n(y)$ is continuous and monotonically decreasing in $|y|$ for $0 \leq |y| \leq y_{\text{waveguide}}$, and $n(y) \equiv n_{\min}$ for $|y| \geq y_{\text{waveguide}}$, see Fig. 2.2. Then (2.19) shows that as $|y|$ increases, so does $\cos \theta$, hence also $|\theta|$. In other words, the rays continuously bend towards the center as they propagate.

Let us denote by θ_0 the angle at which a ray crosses the plane $y \equiv 0$. As before, Eq. (2.19) shows that there is a critical angle $\Theta_{\text{cr}} := \cos^{-1} \left(\frac{n_{\min}}{n_{\max}} \right)$, where $n_{\max} = n(0)$, such that all rays with $|\theta_0| \geq \Theta_{\text{cr}}$ escape to the outer region $|y| > y_{\text{waveguide}}$, where they continue to propagate as straight lines. The paraxial rays for which $|\theta_0| < \Theta_{\text{cr}}$, however, are trapped inside the waveguide. Furthermore, Eq. (2.19) shows that these rays oscillate periodically above and below $y = 0$ as they propagate (Fig. 2.2).

Cylindrical Waveguides (Optical Fibers)

An *optical fiber* is a cylindrical waveguide in which the linear refractive index is a function of $r = \sqrt{x^2 + y^2}$. For example, *step-index fibers* consist of a central glass core, surrounded by a cladding layer whose refractive index is slightly lower than that of the core. In *graded-index fibers*, the refractive index decreases gradually from the fiber center to the boundary [2].

Ray analysis of cylindrical waveguides is similar to that of planar waveguides. Thus, in step-index fibers, the paraxial rays are reflected back by the core-cladding interface. In graded-index fibers, the rays continuously bend toward the fiber center as they propagate. In both cases, the cylindrical waveguide traps the paraxial rays, and the trapping efficiency increases with $\frac{n(r=0)}{n(r=r_f)}$, where r_f is the fiber radius.

2.3 Collimated Beams (Helmholtz Model)

In a homogeneous medium, the eikonal equation reads¹²

$$\nabla S^{(E)} \cdot \nabla S^{(E)} = 1. \quad (2.20)$$

Let us consider this equation with the constant-phase initial condition

$$S^{(E)}(x, y, z = 0) \equiv \alpha, \quad -\infty < x, y < \infty, \quad \alpha \in \mathbb{R}. \quad (2.21)$$

Since both (2.20) and (2.21) are invariant under translations $(x, y) \rightarrow (x + x_0, y + y_0)$, $S^{(E)}$ only depends on z . Therefore, (2.20) reduces to $\frac{dS^{(E)}}{dz} = \pm 1$. In particular, the right-propagating solution is

$$S^{(E)}(x, y, z) = \alpha + z.$$

Since $\nabla S^{(E)} \equiv (0, 0, 1)$, the rays are everywhere parallel to the z -axis, and in particular at $z = 0$. Therefore, the initial condition (2.21) corresponds to a collimated input beam.

Conclusion 2.1 *In the Helmholtz model, a collimated input beam that propagates in the z -direction is represented by the constant-phase initial condition (2.21).*

Indeed, since the rays are perpendicular to the wavefronts, and since a collimated input beam is perpendicular to the (x, y) -plane $z \equiv 0$, this plane has to be a wavefront.

2.4 Fundamental Solution of Helmholtz Equation

We now begin to analyze the Helmholtz equation without applying the geometrical optics approximation (i.e., without neglecting diffraction).

In a homogeneous linear medium, the scalar Helmholtz equation reads

$$\Delta E(\mathbf{x}) + k_0^2 E = 0, \quad \mathbf{x} = (x, y, z). \quad (2.22)$$

¹² We use the notations $S^{(E)}$ and $S^{(\psi)}$ whenever we want to distinguish between the phases of the Helmholtz and Schrödinger solutions, respectively.

In Sect. 1.3 we saw that this equation has plane-wave solutions $E = E_c e^{i\mathbf{k} \cdot \mathbf{x}}$, where $|\mathbf{k}| = k_0$. Equation (2.22) also admits the spherical-wave solution

$$G(\mathbf{x}) = \frac{1}{4\pi\rho} e^{ik_0\rho}, \quad \rho = |\mathbf{x}| = \sqrt{x^2 + y^2 + z^2}. \quad (2.23)$$

Lemma 2.4 *Let G be given by (2.23). Then*

$$\Delta G + k_0^2 G = -\delta(\mathbf{x}),$$

i.e., $\Delta G + k_0^2 G = 0$ for $|\mathbf{x}| > 0$, and $\int_{\mathbb{R}^3} f(\mathbf{x}) (\Delta G + k_0^2 G) d\mathbf{x} = -f(0)$.

Proof Direct differentiation yields

$$G' = \frac{e^{ik_0\rho}}{4\pi} \left(\left(\frac{1}{\rho} \right)' + \frac{ik_0}{\rho} \right), \quad G'' = \frac{e^{ik_0\rho}}{4\pi} \left(\left(\frac{1}{\rho} \right)'' + 2 \left(\frac{1}{\rho} \right)' ik_0 - k_0^2 \right).$$

Therefore,

$$\Delta G + k_0^2 G = G'' + \frac{2}{\rho} G' + k_0^2 G = \frac{e^{ik_0\rho}}{4\pi} \Delta \left(\frac{1}{\rho} \right).$$

Since $\Delta \left(\frac{1}{\rho} \right) = -4\pi\delta(\rho)$, the result follows. \square

If we write $G = A e^{ik_0 S^{(E)}}$, then $A = \frac{1}{4\pi\rho}$ and $S^{(E)} = \rho$. Therefore, the wavefronts of G are the spheres $\rho \equiv \text{constant}$. Since the rays are perpendicular to the wavefronts, they are the lines emanating from $\rho = 0$. We thus see that G describes spherical propagation of radiation from a *point source* at $\rho = 0$.

Exercise 2.4 *Verify that $G(\mathbf{x})$ satisfies relation (2.14), i.e., that the power in the intersection of a cone of rays that starts at $\rho = 0$ with a sphere of radius ρ , is independent of ρ .*

The Helmholtz equation (2.22) also admits the spherical-wave solution

$$G_-(\mathbf{x}) = \frac{1}{4\pi\rho} e^{-ik_0\rho}, \quad \rho = \sqrt{x^2 + y^2 + z^2}. \quad (2.24)$$

In this case, $A = \frac{1}{4\pi\rho}$ and $S^{(E)} = -\rho$. Therefore, the wavefronts of G_- are the spheres $\rho \equiv \text{constant}$, and the rays are the lines pointing towards $\rho = 0$.¹³ Hence, expression (2.24) describes a *point sink* located at $\rho = 0$.

¹³ Recall that $S^{(E)}$ increases in the direction of propagation of the ray (Sect. 2.1.1).

2.5 Focused Beams (Helmholtz Model)

In many applications, the incoming laser beam is focused by a lens. To represent the effect of a lens on an input beam, we first note that the solution of Helmholtz equation (2.22) with a point sink located at $(0, 0, F)$ is

$$G_- = \frac{1}{4\pi\sqrt{x^2 + y^2 + (z - F)^2}} e^{ik_0 S^{(E)}}, \quad (2.25a)$$

where

$$S^{(E)} = -\sqrt{x^2 + y^2 + (z - F)^2}. \quad (2.25b)$$

Hence, the rays are the lines pointing towards $(0, 0, F)$. In particular, all the rays that start at the (x, y) -plane $z \equiv 0$ intersect at $(0, 0, F)$. Therefore, expression (2.25b) describes the phase of a beam which is focused at $z = 0$ by a lens with focal point at $(0, 0, F)$. In particular, the phase at $z = 0$ is

$$k_0 S^{(E)}(x, y, 0) = -k_0 \sqrt{x^2 + y^2 + F^2}. \quad (2.26)$$

Conclusion 2.2 *In the Helmholtz model, a lens located at $z = 0$ with a focal point at $(0, 0, F)$ is represented by the phase term (2.26).*

Indeed, the solution of the eikonal equation (2.20) with the initial condition (2.26) is given by (2.25b).

Exercise 2.5 *Derive expression (2.26) from the condition that all the rays that emanate from the (x, y) -plane $z \equiv 0$ should reach the focal point $(0, 0, F)$ with the same travel time (phase), so that they would interfere constructively.*

The representation of a lens in an inhomogeneous or nonlinear medium is also given by (2.26). Indeed, although we derived this expression for a linear homogeneous medium, the lens effect is independent of the subsequent propagation. Of course, if the medium is inhomogeneous or nonlinear, the lens will not focus all rays to the point $(0, 0, F)$.¹⁴

2.6 Singularity in the Helmholtz Model

We now show that under the geometrical optics approximation, solutions of the Helmholtz equation can become singular:

¹⁴ Even in a linear homogeneous medium, if we do not apply the geometrical optics approximation, the lens does not focus the solution to a point (Sect. 2.10).

Lemma 2.5 *Consider the Helmholtz equation (2.22) for propagation in a homogeneous linear medium. Then under the geometrical optics approximation, a focused incoming beam has a δ -function singularity at the focal point.*

Proof Under the geometrical optics approximation, the phase evolves according to the eikonal equation. In Sect. 2.5 we saw that the initial phase is given by (2.26), and the corresponding solution of the eikonal equation (2.20) is $S^{(E)} = -\sqrt{x^2 + y^2 + (z - F)^2}$. Therefore, all rays that start at the (x, y) -plane $z \equiv 0$ intersect at the focal point $(0, 0, F)$. Hence, by Corollary 2.1, all the beam power concentrates at the focal point. \square

It is not really surprising that the solution becomes singular at the focal point, since under the geometrical optics approximation, a lens focuses all the rays into a single point, and classical solutions break down whenever their characteristics intersect. For example, in hyperbolic equations, the crossing of characteristics corresponds to a shock wave (see, e.g., [157]). Note, however, that our analysis also reveals that the singularity is of a delta-function type, whereby all the solution power concentrates at the focal point. In particular, the solution becomes infinite at the singularity point. This is different from hyperbolic shock waves, where only the derivative becomes infinite when the characteristics intersect.

2.7 Global Existence in the Linear Helmholtz Equation in the Half Space

In the scalar linear Helmholtz equation (2.22), under the geometrical optics approximation, a focused input beam become singular at the focal point (Lemma 2.5). Since physical quantities do not become singular, we would like to know which approximation is “responsible” for this singularity.¹⁵

Equation (2.22) is already an approximate model, since it neglects the vectorial nature of the electric field (Sect. 1.2). We now show that when Eq. (2.22) is driven by right-propagating incoming beam at $z = 0$, its solution exists for all $z > 0$. Therefore, the singularity in Lemma 2.5 is not due to approximations made in the derivation of the scalar Helmholtz equation, but rather due to the geometrical optics approximation.

Consider the Helmholtz equation in the positive half space

$$\Delta E(x, y, z) + k_0^2 E = 0, \quad z > 0, \quad -\infty < x, y < \infty, \quad (2.27)$$

¹⁵ This book is mainly concerned with singular NLS solutions. Therefore, understanding the origin of singularities in the linear case will help us to determine whether NLS singularity is a linear or a nonlinear phenomenon.

with a right-propagating incoming beam, whose value at $z = 0$ is $E_0^{\text{inc}}(x, y)$.¹⁶ To solve this problem, we first write the incoming beam as

$$E_0^{\text{inc}}(x, y) = \frac{1}{2\pi} \int \widehat{E_0^{\text{inc}}}(k_x, k_y) e^{i(k_x x + k_y y)} dk_x dk_y.$$

The corresponding right-propagating solution of (2.27) is, see (1.13),

$$E(x, y, z) = \frac{1}{2\pi} \int \widehat{E_0^{\text{inc}}}(k_x, k_y) e^{i(k_x x + k_y y + \sqrt{k_0^2 - k_x^2 - k_y^2} z)} dk_x dk_y. \quad (2.28)$$

Lemma 2.6 *Assume that $E_0^{\text{inc}}(x, y)$ is sufficiently smooth and decays sufficiently fast to zero as $\sqrt{x^2 + y^2} \rightarrow \infty$. Then expression (2.28) is smooth and bounded for all $z > 0$.*

Proof Recall that the decay rate of Fourier coefficients as $\sqrt{k_x^2 + k_y^2} \rightarrow \infty$ increases with the smoothness of the function. Therefore, since $E_0^{\text{inc}}(x, y)$ is sufficiently smooth and decays sufficiently fast to zero as $\sqrt{x^2 + y^2} \rightarrow \infty$, $\widehat{E_0^{\text{inc}}}(k_x, k_y)$ is also sufficiently smooth and decays sufficiently fast as $\sqrt{k_x^2 + k_y^2} \rightarrow \infty$. Hence, so does $\hat{E}(k_x, k_y, z) = \widehat{E_0^{\text{inc}}}(k_x, k_y) e^{i(\sqrt{k_0^2 - k_x^2 - k_y^2} z)}$. Therefore, $E(x, y, z)$ exists and is bounded for all z . \square

Corollary 2.2 *Let the scalar linear Helmholtz equation (2.27) be driven at $z = 0$ by a focused incoming beam which is smooth and decays sufficiently fast to zero as $\sqrt{x^2 + y^2} \rightarrow \infty$. Then the solution does not become singular.*

Comparison of Lemma 2.5 with Corollary 2.2 leads to

Conclusion 2.3 *The singularity in Lemma 2.5 is due to the geometrical optics approximation.*

Remark The spherical wave G_- , see (2.25), is a solution of Helmholtz equation with the focused incoming beam

$$E_0^{\text{inc}}(x, y) = G_-(x, y, z = 0) = \frac{1}{4\pi \sqrt{x^2 + y^2 + F^2}} e^{-ik_0 \sqrt{x^2 + y^2 + F^2}}. \quad (2.29)$$

Since this solution becomes singular at $(0, 0, F)$, it appears to be a “counter-example” to Corollary 2.2. In Sect. 34.7 we shall see, however, that physical solutions of Helmholtz equation that are driven at $z = 0$ by a right-propagating incoming beam, should propagate to the right as $z \rightarrow +\infty$. The spherical wave G_- , however, propagates to the left as $z \rightarrow +\infty$. Thus, the resolution of this “contradiction” is that the

¹⁶ The discussion here is very informal. The formulation of boundary conditions for the Helmholtz equation in the positive half space will be discussed in Sect. 34.7.

solution of Helmholtz equation with the incoming beam (2.29) is non-unique. The unique physical solution that satisfies the *radiation-to-the-right boundary condition* as $z \rightarrow +\infty$ exists globally and is bounded, but solutions that do not satisfy this radiation boundary condition may become unbounded.

2.8 Representations of Input Beams

2.8.1 Relation Between $S^{(E)}$ and $S^{(\psi)}$

Let $E(x, y, z)$ be a solution of Helmholtz equation (2.22). As in Sect. 1.3, if we substitute $E = e^{ik_0 z} \psi(x, y, z)$ and apply the paraxial approximation, then ψ satisfies the Schrödinger equation

$$2ik_0 \psi_z(x, y, z) + \Delta_{\perp} \psi = 0, \quad \Delta_{\perp} = \frac{\partial^2}{\partial x^2} + \frac{\partial^2}{\partial y^2}. \quad (2.30)$$

In Sect. 2.1.1 we decomposed the Helmholtz solution as

$$E = A(x, y, z) e^{ik_0 S^{(E)}(x, y, z)},$$

where A and $S^{(E)}$ are real. Similarly, we can decompose the Schrödinger solution as

$$\psi = A(x, y, z) e^{ik_0 S^{(\psi)}(x, y, z)},$$

where A and $S^{(\psi)}$ are real. Since $E = e^{ik_0 z} \psi$, the amplitudes of E and ψ are the same, but their phases are not. Rather, they are related through

$$k_0 S^{(E)} = k_0 z + k_0 S^{(\psi)}. \quad (2.31)$$

The paraxial approximation implies that $k_0 S^{(\psi)}$ is slowly-varying in z , compared with $k_0 z$. Therefore,

$$\frac{\partial}{\partial z} S^{(\psi)} \ll 1. \quad (2.32)$$

In Sects. 2.8.2, 2.8.4, and 2.8.5 we will use relation (2.31) to find the representations of collimated, focused, and tilted input beams in the Schrödinger model, from their respective representations in the Helmholtz model.

2.8.2 Collimated Beams (Schrödinger Model)

In Conclusion 2.1 we saw that in the Helmholtz model, a collimated input beam is represented by the constant-phase initial condition $S^{(E)}(z = 0) \equiv \alpha$. Therefore, by relation (2.31) we have

Conclusion 2.4 *In the Schrödinger model, a collimated input beam that propagates in the z -direction is represented by the constant-phase initial condition*

$$S^{(\psi)}(x, y, z = 0) \equiv \alpha, \quad -\infty < x, y < \infty, \quad \alpha \in \mathbb{R}.$$

Corollary 2.3 *If the initial condition ψ_0 of the Schrödinger equation is real, then it corresponds to a collimated input beam that propagates in the z -direction.*

2.8.3 From Spherical to Parabolic Waves

Consider the spherical-wave solution G . Since the phase of G is $k_0 S^{(E)} = k_0 \rho$, see (2.23), the corresponding phase of ψ is

$$k_0 S^{(\psi)} = k_0(\rho - z).$$

Let us consider the narrow paraxial portion of the spherical-wave solution G that propagates in the direction of the positive z -axis. Then $x, y \ll z$, and so we can approximate

$$\rho = (x^2 + y^2 + z^2)^{\frac{1}{2}} = z \left(1 + \frac{x^2 + y^2}{z^2} \right)^{\frac{1}{2}} \approx z \left(1 + \frac{1}{2} \frac{x^2 + y^2}{z^2} \right).$$

Hence,

$$S^{(\psi)}(x, y, z) \approx \frac{r^2}{2z}, \quad r = \sqrt{x^2 + y^2}, \quad (2.33)$$

i.e., the wavefronts of ψ are parabolic.

Conclusion 2.5 *Under the paraxial approximation, a spherical wave turns into a parabolic one.*

For that reason, the *paraxial approximation* is also called the *parabolic approximation*.

2.8.4 Focused Beams (Schrödinger Model)

In order to represent a focusing lens ($F > 0$) in the Schrödinger model, let $G_- = e^{ik_0 z} \psi$, where G_- is given by (2.25). Since $S^{(E)}$ is given by (2.25b), then by (2.31), for $0 < z < F$,

$$S^{(\psi)} = -\sqrt{x^2 + y^2 + (z - F)^2} - z = (z - F) \sqrt{1 + \frac{r^2}{(z - F)^2}} - z. \quad (2.34)$$

Application of the paraxial approximation $r \ll z - F$ gives $\left(1 + \frac{r^2}{(z-F)^2}\right)^{\frac{1}{2}} \approx 1 + \frac{r^2}{2(z-F)^2}$. Therefore,

$$S^{(\psi)}(x, y, z) \approx \frac{r^2}{2(z-F)} - F.$$

Since a constant phase term has no effect, we can also write

$$S^{(\psi)}(x, y, z) \approx \frac{r^2}{2(z-F)}. \quad (2.35)$$

In particular, the phase at $z = 0$ is

$$k_0 S^{(\psi)}(x, y, 0) \approx -k_0 \frac{r^2}{2F}. \quad (2.36)$$

Therefore, we have

Conclusion 2.6 *In the Schrödinger model (2.30), a lens located at $z = 0$ whose focal point is at $(0, 0, F)$, is represented by adding a quadratic phase term to the initial condition as follows:*

$$\underbrace{\psi_0(x, y)}_{\text{no lens}} \rightarrow \underbrace{\psi_0(x, y)e^{-ik_0 \frac{r^2}{2F}}}_{\text{with lens}}. \quad (2.37)$$

As expected, the addition of a lens does not affect the input beam amplitude $|\psi_0|$.

Remark The dimensionless representation of a lens is given in Conclusion 2.12.

2.8.5 Tilted Beams

We can use a similar approach to find the representation of a tilted input beam, i.e., a collimated input beam whose direction of propagation is not parallel to the z -axis. Recall that the Helmholtz equation (2.22) admits the plane-wave solution $E = E_c e^{i(k_x x + k_y y + k_z z)}$, where $k_x^2 + k_y^2 + k_z^2 = k_0^2$. This solution can be written as $E = E_c e^{ik_0(n_x x + n_y y + n_z z)}$, where $\mathbf{n} = (n_x, n_y, n_z)$ is the unit vector in the direction of propagation ($n_x^2 + n_y^2 + n_z^2 = 1$). For this plane wave, $S^{(E)} = n_x x + n_y y + n_z z$. Hence, for the corresponding Schrödinger solution

$$S^{(\psi)}(x, y, z) = S^{(E)} - z = n_x x + n_y y + (n_z - 1)z.$$

In particular,

$$S^{(\psi)}(x, y, 0) = n_x x + n_y y.$$

In fact, in Sect. 2.12.3 we will see that the correct expression is¹⁷

$$S^{(\psi)}(x, y, 0) = \frac{n_x}{n_z} x + \frac{n_y}{n_z} y.$$

Since in paraxial propagation $n_z = 1 + O(f^2)$, see (2.66), these two expressions for $S^{(\psi)}(x, y, 0)$ are equivalent, up to the $O(f^2)$ accuracy of the paraxial Schrödinger model (Sect. 2.12.1).¹⁸

Conclusion 2.7 *In the Schrödinger model (2.30), a tilt of the input beam in the direction of the unit vector $\mathbf{n} = (n_x, n_y, n_z)$ is represented by adding a linear phase term to the initial condition, as follows:*

$$\underbrace{\psi_0(x, y)}_{\text{no tilt}} \rightarrow \underbrace{\psi_0(x, y) e^{ik_0(\frac{n_x}{n_z}x + \frac{n_y}{n_z}y)}}_{\text{with tilt}}.$$

Remark The tilt angle θ is given by $\tan \theta = \frac{|\mathbf{n}_\perp|}{|n_z|}$, where $\mathbf{n}_\perp = (n_x, n_y)$.

Remark The dimensionless expression for a tilted beam is given in Conclusion 2.13.

Exercise 2.6 *Analyze the effect of the phase in the initial condition*

$$\psi_0(x) = e^{-\left(\frac{x}{\xi}\right)^2} e^{ik_0 \log(e^x + e^{-x})}.$$

2.8.6 Vortex Beams

The Helmholtz equation (2.22) admits solutions of the form

$$E(z, r, \theta) = e^{im\theta} A(z, r),$$

where (z, r, θ) are the cylindrical coordinates, m is an integer, and A is the solution of

$$A_{zz} + A_{rr} + \frac{1}{r} A_r + \left(k_0^2 - \frac{m^2}{r^2}\right) A = 0.$$

¹⁷ That this is the correct expression will follow from Galilean invariance of the Schrödinger equation.

¹⁸ The quadratic phase term (2.35) for the effect of a lens in the Schrödinger model is also not equal to $S^{(E)} - z$, see (2.34). It is, however, $O(f^2)$ equivalent to it, since under the paraxial approximation $\frac{r}{z-F} = O(f)$, see (2.64). We “prefer” approximation (2.35) over the “exact” expression (2.34), because (2.35) agrees with the lens transformation of the linear Schrödinger equation (Corollary 8.1).

These solutions are called *vortex solutions*, because they rotate around the z -axis as they propagate in the z -direction.¹⁹ Indeed, if $A(z, r)$ is real, then the equal-phase curves in the (r, θ) -plane are $m\theta \equiv \text{constant}$, i.e., lines emanating from $r = 0$. Since the rays are perpendicular to these lines, they point in the azimuthal direction.

By (2.31), the initial phase of the corresponding Schrödinger solution is $\arg \psi(x, y, 0) = m\theta$. Therefore we have

Conclusion 2.8 *In the Schrödinger model (2.30), a rotation of the incoming beam around the z -axis is represented by adding the phase-term $e^{im\theta}$ to the initial condition, as follows:*

$$\underbrace{\psi_0(x, y)}_{\text{no rotation}} \rightarrow \underbrace{\psi_0(x, y)e^{im\theta}}_{\text{with rotation}}.$$

2.8.7 Generic Input Beams

We can summarize the results of Sect. 2.8, as follows. In the dimensional Schrödinger model (2.30):

1. A collimated input beam that propagates in the z -direction is represented by a real initial condition ψ_0 .
2. A focused input beam that propagates in the z -direction is represented by

$$\psi_0 = A_0(x, y)e^{-ik_0 \frac{r^2}{2F}}, \quad (2.38)$$

where $A_0(x, y) = |\psi_0(x, y)|$ is the input beam amplitude and F is the focal length.

3. A tilted collimated input beam that propagates in the direction of the unit vector $\mathbf{n} = (n_x, n_y, n_z)$ is represented by

$$\psi_0 = A_0(x, y)e^{ik_0 \left(\frac{n_x}{n_z}x + \frac{n_y}{n_z}y \right)}.$$

4. A tilted focused input beam that propagates in the direction of the unit vector $\mathbf{n} = (n_x, n_y, n_z)$ is represented by

$$\psi_0 = A_0(x, y)e^{-ik_0 \frac{r^2}{2F}} e^{ik_0 \left(\frac{n_x}{n_z}x + \frac{n_y}{n_z}y \right)}. \quad (2.39)$$

5. A vortex input beam that propagates in the z -direction is represented by

$$\psi_0 = A_0(x, y)e^{im\theta}, \quad m = \pm 1, \pm 2, \dots$$

¹⁹ Vortex solutions are studied in Chaps. 15 and 20 and in Sects. 23.7 and 24.7.

2.9 Geometrical Optics Analysis of Paraxial Propagation

In Sect. 1.3 we saw that under the paraxial approximation, the Helmholtz equation (2.22) reduces to the Schrödinger equation (2.30). We now analyze the Schrödinger equation under the geometrical optics approximation.

Substituting $\psi = Ae^{ik_0 S^{(\psi)}}$ in (2.30), where A and $S^{(\psi)}$ are real, gives

$$\begin{aligned} -2k_0^2 AS_z^{(\psi)} - 2ik_0 A_z + \Delta_\perp A + 2ik_0 \nabla_\perp A \cdot \nabla_\perp S^{(\psi)} \\ + A \left(-k_0^2 (\nabla_\perp S^{(\psi)})^2 + ik_0 \Delta_\perp S^{(\psi)} \right) = 0, \end{aligned}$$

where $\nabla_\perp = \left(\frac{\partial}{\partial x}, \frac{\partial}{\partial y} \right)$ and $\Delta_\perp = \frac{\partial^2}{\partial x^2} + \frac{\partial^2}{\partial y^2}$. The equation for the real parts, after division by $k_0^2 A$, is

$$2S_z^{(\psi)} + \left(\nabla_\perp S^{(\psi)} \right)^2 - \frac{1}{k_0^2} \frac{\Delta_\perp A}{A} = 0. \quad (2.40a)$$

Similarly, the equation for the imaginary parts, after multiplication by A , is

$$\left(A^2 \right)_z + \nabla_\perp S^{(\psi)} \cdot \nabla_\perp \left(A^2 \right) + A^2 \Delta_\perp S^{(\psi)} = 0. \quad (2.40b)$$

When $k_0 \gg 1$, we can apply the geometrical optics approximation and neglect the diffraction term $\Delta_\perp A$. In this case, (2.40a) becomes

$$2S_z^{(\psi)} + \left(\nabla_\perp S^{(\psi)} \right)^2 = 0. \quad (2.41)$$

Equation (2.41) is the *paraxial eikonal equation* in a homogeneous medium, as is confirmed in the following exercise:

Exercise 2.7 Derive (2.41) from the eikonal equation for a homogeneous medium (2.4), by using relation (2.31) and the paraxial approximation (2.32).

Unlike Eq. (2.40a), Eq. (2.40b) remains unchanged under the geometrical optics approximation. Equation (2.40b) is the *paraxial transport equation* in a homogeneous medium, as is confirmed in the following exercise:

Exercise 2.8 Derive (2.40b) from the transport equation (2.13), by using relation (2.31) and the paraxial approximation (2.32).

In Sect. 2.1 we saw that the eikonal and transport equations have the same characteristics. Interestingly, the characteristics of the paraxial eikonal and transport equations are not the same. Rather, they are given by

$$\frac{dz}{d\sigma} = 2, \quad \frac{dx}{d\sigma} = S_x^{(\psi)}, \quad \frac{dy}{d\sigma} = S_y^{(\psi)},$$

and

$$\frac{dz}{d\sigma} = 1, \quad \frac{dx}{d\sigma} = S_x^{(\psi)}, \quad \frac{dy}{d\sigma} = S_y^{(\psi)}, \quad (2.42)$$

respectively.

Exercise 2.9 Derive (2.42) for the characteristics of the paraxial transport equation from Eq. (2.7) for the characteristics of the transport equation, by using relation (2.31) and the paraxial approximation (2.32).

Let ψ_0 be the generic focused input beam (2.38). Then the corresponding initial conditions for $S^{(\psi)}$ and A^2 are

$$S^{(\psi)}(x, y, 0) = -\frac{r^2}{2F} \quad (2.43a)$$

and

$$A^2(x, y, 0) = |\psi_0(x, y)|^2. \quad (2.43b)$$

It is easy to verify that the solution of the paraxial eikonal equation (2.41), subject to the initial condition (2.43a), is²⁰

$$S^{(\psi)} = \frac{r^2}{2(z - F)}. \quad (2.44)$$

Substituting (2.44) in the paraxial transport equation (2.40b) gives

$$\left(A^2\right)_z + \frac{1}{z - F}(x, y) \cdot \nabla_{\perp} \left(A^2\right) + \frac{2}{z - F} A^2 = 0. \quad (2.45)$$

The solution of this equation, subject to the initial condition (2.43b), can be calculated by the method of characteristics, yielding

$$A^2(x, y, z) = \frac{1}{L^2(z)} \left| \psi_0 \left(\frac{x}{L(z)}, \frac{y}{L(z)} \right) \right|^2, \quad L(z) = 1 - \frac{z}{F}.$$

Here $L(z)$ is the beam width, and $L^{-1}(z)$ is proportional to the on-axis amplitude $A(0, 0, z) = |\psi(0, 0, z)|$.

Let $\psi_{go} := Ae^{ik_0 S^{(\psi)}}$, where A and $S^{(\psi)}$ are the solutions of (2.40b) and (2.41), respectively.²¹ Then

²⁰ We already derived this expression by applying the geometrical optics approximation and then the paraxial approximation, see (2.35). In the derivation here the order of the approximations is reversed.

²¹ The subscript *go* emphasizes that ψ_{go} is not an exact solution of the Schrödinger equation, as it is obtained under the geometrical optics approximation.

$$\psi_{\text{go}}(x, y, z) = \frac{1}{L(z)} \left| \psi_0 \left(\frac{x}{L}, \frac{y}{L} \right) \right| e^{ik_0 \frac{r^2}{2(z-F)}}, \quad L(z) = 1 - \frac{z}{F}. \quad (2.46)$$

Expression (2.46) with $F > 0$ describes the propagation of a focused input beam under the paraxial and geometrical optics approximations. In particular, the beam width $L(z)$ decreases linearly with z , and vanishes at the focal point $z = F$. Moreover,

$$|\psi_{\text{go}}|^2 = \frac{1}{L^2(z)} \left| \psi_0 \left(\frac{x}{L}, \frac{y}{L} \right) \right|^2 \rightarrow P \cdot \delta(\mathbf{x}), \quad z \rightarrow F-, \quad (2.47)$$

where $P = \int |\psi_0|^2 dx dy$ is the input power, and the limit is in the sense of distributions.

Lemma 2.7 *In the linear Schrödinger model, under the geometrical optics approximation, a focusing lens leads to a δ -function singularity at the focal point.*

Remark Lemma 2.7 is the paraxial analog of Lemma 2.5.

Remark The singularity in Lemma 2.7 is not related to non-smoothness or insufficient decay at infinity of the initial condition, as it occurs e.g., for a focused Gaussian input beam.

Remark See Sect. 38.8 for a continuation of ψ_{go} beyond the singularity.

2.10 Arrest of Linear Collapse by Diffraction (Gaussian Beams)

In Lemma 2.7 we saw that in the linear Schrödinger model, under the geometrical optics approximation, a focused input beam becomes singular at the lens focal point. We now show that if one does not apply the geometrical optics approximation (i.e., when diffraction is not neglected in the Schrödinger model), the focused beam does not collapse to a point. Rather, it narrows down to a positive *diffraction-limited width*, and then spreads out with further propagation.

Our starting point is the linear Schrödinger equation (2.30). As in the diffractionless case (Sect. 2.9), let $\psi = A e^{ik_0 S^{(\psi)}}$, where A and $S^{(\psi)}$ are real. Therefore, A and $S^{(\psi)}$ are solutions of

$$2S_z^{(\psi)} + \left(\nabla_{\perp} S^{(\psi)} \right)^2 - \frac{1}{k_0^2} \frac{\Delta_{\perp} A}{A} = 0, \quad (2.48a)$$

and

$$\left(A^2 \right)_z + \nabla_{\perp} S^{(\psi)} \cdot \nabla_{\perp} \left(A^2 \right) + A^2 \Delta_{\perp} S^{(\psi)} = 0, \quad (2.48b)$$

respectively, see (2.40). Unlike the analysis in Sect. 2.9, here we do not neglect the diffraction term $\Delta_{\perp} A$.

In general, Eqs. (2.48) cannot be solved explicitly. An explicit solution can be obtained, however, for the focused Gaussian input beam²²

$$\psi_0(x, y) = E_c e^{-\frac{r^2}{2r_0^2} - i \frac{k_0 r^2}{2F}}, \quad r = \sqrt{x^2 + y^2},$$

where F is the focal distance and r_0 is the input beam width. By (2.43), the initial conditions for (2.48) are

$$S^{(\psi)}(x, y, 0) = -\frac{r^2}{2F}, \quad A^2(x, y, 0) = E_c^2 e^{-\frac{r^2}{r_0^2}}. \quad (2.48c)$$

Let us look for a solution of (2.48) of the form

$$S^{(\psi)} = \frac{a(z)r^2}{2} + \zeta(z), \quad A^2 = \frac{E_c^2}{L^2(z)} e^{-\frac{r^2}{r_0^2 L^2(z)}}, \quad (2.49)$$

i.e., for a solution that maintains a self-similar Gaussian profile during its propagation.

Exercise 2.10 *Verify that the self-similar Gaussian ansatz (2.49) is an exact solution of (2.48), provided that $a(z)$, $\zeta(z)$, and $L(z)$ satisfy*

$$a^2 + a_z = \frac{1}{k_0^2 r_0^4} \frac{1}{L^4}, \quad \zeta_z = -\frac{1}{k_0^2 r_0^2} \frac{1}{L^2}, \quad a = \frac{L_z}{L}, \quad (2.50)$$

subject to the initial conditions

$$a(0) = -\frac{1}{F}, \quad \zeta(0) = 0, \quad L(0) = 1.$$

Thus, the assumption that the solution maintains a self-similar Gaussian profile is fully consistent with the linear Schrödinger equation (2.30).²³

Substitution (2.49) allows us to replace a PDE (the Schrödinger equation) with a system of ODEs.²⁴ In general, it is considerably simpler to analyze ODEs than a PDE. Moreover, the ODEs (2.50) can be explicitly solved, as follows. Since $a = L_z/L$, then

²² The assumption that the input beam has a Gaussian profile is common in optics.

²³ This is not the case in nonlinear propagation of Gaussian input beams (Sect. 3.5). Even in linear propagation, this *aberrationless propagation* property holds only for Gaussian profiles. Thus, for example, if the input beam has a *sech* profile, the beam does not maintain a *sech* profile during linear propagation. The reason why this aberrationless property only holds for linear Gaussian beams will become clear in Sect. 2.15.3.

²⁴ This is possible because the transverse profile of the solution is “known” to be a rescaled Gaussian.

$$a^2 + a_z = \frac{L_{zz}}{L}.$$

Therefore, the dynamics of $L(z)$ is governed by

$$L_{zz}(z) = \frac{1}{L_{\text{diff}}^2} \frac{1}{L^3}, \quad (2.51a)$$

where $L_{\text{diff}} = k_0 r_0^2$ is the *diffraction length*.²⁵ The initial conditions for (2.51a) are

$$L(0) = 1, \quad L_z(0) = a(0)L(0) = -\frac{1}{F}. \quad (2.51b)$$

Since a converging, collimated, or diverging beam corresponds to $F > 0$, $F = \infty$, or $F < 0$, respectively, from (2.51b) we have

Conclusion 2.9 *An input beam is collimated when $L_z(0) = 0$, converging (focused) when $L_z(0) < 0$, and diverging (defocused) when $L_z(0) > 0$.*

This conclusion is intuitive since, for example, a beam is focused if and only if its width L is decreasing.

The solution of (2.51) follows from

Lemma 2.8 *The solution of*

$$L_{zz}(z) = \frac{K}{L^3}, \quad L(0) = L_0 > 0, \quad L_z(0) = L'_0, \quad (2.52)$$

where K is a constant, is given by

$$L^2(z) = c_1 \left(z + \frac{L_0 L'_0}{c_1} \right)^2 + \frac{K}{c_1}, \quad c_1 = (L'_0)^2 + \frac{K}{L_0^2}. \quad (2.53)$$

This solution can also be written as

$$L^2(z) = c_1 z^2 + 2L_0 L'_0 z + L_0^2, \quad (2.54)$$

and as

$$L^2(z) = (L_0 + zL'_0)^2 + \frac{K}{L_0^2} z^2. \quad (2.55)$$

Proof Multiplying (2.52) by $2L_z$ and integrating gives

$$(L_z)^2 = \frac{-K}{L^2} + c_1, \quad c_1 = (L'_0)^2 + \frac{K}{L_0^2}.$$

²⁵ See Sect. 2.11.

If we multiply this equation by L^2 we can rewrite it as

$$\frac{1}{2}y_z = \pm\sqrt{c_1y - K}, \quad y := L^2,$$

where the \pm sign corresponds to the sign of L'_0 . Integrating this equation and using the initial conditions gives

$$\frac{1}{c_1}\sqrt{c_1y - K} = \pm z + \frac{L_0|L'_0|}{c_1} = \text{sign}(L'_0) \left(z + \frac{L_0L'_0}{c_1} \right),$$

which leads to (2.53). □

In the case of Eq. (2.51),

$$K = \frac{1}{L_{\text{diff}}^2}, \quad L_0 = 1, \quad L'_0 = -\frac{1}{F}.$$

Therefore, by (2.55), the solution of (2.51) is

$$L^2(z) = \left(1 - \frac{z}{F}\right)^2 + \left(\frac{z}{L_{\text{diff}}}\right)^2. \quad (2.56)$$

The first and second terms on the right-hand side correspond to focusing (or defocusing) by the lens and to defocusing due to diffraction, respectively.

We can rewrite the solution of (2.51) as, see (2.53),

$$L^2(z) = \left(\frac{1}{F^2} + \frac{1}{L_{\text{diff}}^2}\right) (z - z_{\min})^2 + L_{\min}^2, \quad (2.57)$$

where

$$z_{\min} = \frac{F}{1 + F^2/L_{\text{diff}}^2}, \quad L_{\min} = \frac{F}{\sqrt{F^2 + L_{\text{diff}}^2}}.$$

Expression (2.57) shows that $L(z)$ does not shrink to zero at any $z > 0$.

Corollary 2.4 *Diffraction arrests collapse of focused Gaussian input beams in paraxial linear propagation.*

Equation (2.57) also shows that when $F > 0$, the beam focuses for $0 < z < z_{\min}$, and defocuses for $z > z_{\min}$. The minimal value of L is $L_{\min} > 0$. It is attained at $z = z_{\min} < F$, i.e., before the focal point (Fig. 2.3).

Let us consider the case where the focusing lens is much stronger than diffraction (*tight focusing*), i.e., $0 < F \ll L_{\text{diff}}$. In this case, $z_{\min} \approx F$ and $L_{\min} \approx F/L_{\text{diff}}$.

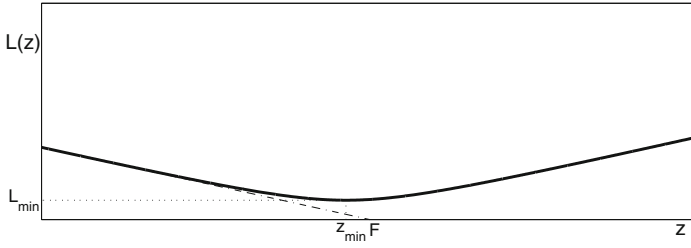


Fig. 2.3 The collapse of a focused input beam under the geometrical optics approximation in linear propagation (*dashed line*), is arrested by diffraction (*solid line*)

Since the dimensional beam width is $r_0 L(z)$, see (2.49), the minimal dimensional beam width (*diffraction-limited width*) is

$$r_{\min} = r_0 L_{\min} \approx \frac{F}{k_0 r_0} = \frac{\lambda}{2\pi} \frac{F}{r_0}.$$

Remark One of the earliest indications that propagation of intense laser beams in a bulk medium is nonlinear, was provided by the experiments of Hercher, in which high-power laser beams that propagated in glass created thin threads of damage, whose widths were well below the diffraction-limited widths expected in linear propagation. See Sect. 3.3.1 for further details.

2.11 Diffraction Length (L_{diff})

We now consider the physical meaning of the diffraction length (also called the *Rayleigh length*) $L_{\text{diff}} := k_0 r_0^2$, which appeared in the derivation of (2.51a). We first note that since $k_0 = 2\pi/\lambda$ has units of 1/length, L_{diff} has units of length. It is also easy to see that L_{diff} is the characteristic length scale of z in (2.51a).²⁶ In addition, the solution of (2.51) with a collimated Gaussian input beam ($F = \infty$, $L_z(0) = 0$) is, see (2.56),

$$L^2(z) = 1 + \left(\frac{z}{L_{\text{diff}}} \right)^2.$$

For comparison, in the absence of diffraction (i.e., under the geometrical optics approximation), the beam remains collimated, and so $L^2(z) \equiv 1$.

Conclusion 2.10 *The diffraction length $L_{\text{diff}} := k_0 r_0^2$ is the characteristic distance for diffraction effects, i.e., the characteristic propagation distance over which the beam width undergoes $O(1)$ changes because of diffraction.*

²⁶ Indeed, under the rescaling $\tilde{z} = z/L_{\text{diff}}$, (2.51a) reads $L_{\tilde{z}\tilde{z}} = L^{-3}$, and so $[L_{\tilde{z}\tilde{z}}] = O(1)$.

In other words, L_{diff} is the characteristic distance at which neighboring rays begin to interact with each other, so that the validity of the geometrical optics approximation breaks down.

We can also derive the expression for L_{diff} from a dimensional argument.²⁷ Consider the Schrödinger equation

$$2ik_0\psi_z + \psi_{xx} + \psi_{yy} = 0.$$

If we change to the dimensionless variables

$$\tilde{x} = \frac{x}{r_0}, \quad \tilde{y} = \frac{y}{r_0}, \quad \tilde{z} = \frac{z}{Z}, \quad \tilde{\psi} = \frac{\psi}{E_c},$$

where r_0 and Z are the characteristic length-scales in the transverse and axial directions, respectively, and E_c is the characteristic magnitude of ψ , we get

$$2ik_0 \frac{E_c}{Z} \tilde{\psi}_{\tilde{z}} + \frac{E_c}{r_0^2} [\tilde{\psi}_{\tilde{x}\tilde{x}} + \tilde{\psi}_{\tilde{y}\tilde{y}}] = 0. \quad (2.58)$$

The diffraction length is the distance Z at which diffraction has an $O(1)$ effect, i.e., $\tilde{\psi}_{\tilde{z}} = O(1)$. This occurs when the two terms in (2.58) are of comparable magnitudes, i.e.,

$$\frac{k_0 E_c}{Z} = \frac{E_c}{r_0^2}.$$

Therefore, $Z = k_0 r_0^2$.

Exercise 2.11 Calculate the diffraction length for an input beam with wavelength $\lambda = 0.5 \mu\text{m}$ and width $r_0 = 1 \text{ cm}$.

In Observation 1.2 we noted that the width of a laser beam is typically much larger than its wavelength (i.e., $r_0 \gg \lambda$). Therefore, there are *three distinct length-scales* in paraxial propagation:

$$\lambda \ll r_0 = [x], [y] \ll L_{\text{diff}} = [z].$$

The ratios between these three length-scales are characterized, however, by a *single* nondimensional parameter, since

$$\frac{\lambda}{r_0} = 2\pi f \quad \text{and} \quad \frac{r_0}{L_{\text{diff}}} = f,$$

²⁷ This approach has the advantage that it applies also to non-Gaussian beams.

where

$$f := \frac{1}{r_0 k_0} \ll 1, \quad (2.59)$$

is the *nonparaxiality parameter*.²⁸

Remark As noted, the characteristic length-scales in x and y are significantly smaller than in z . This anisotropy has nothing to do with the medium, which is assumed to be homogeneous and isotropic. Rather, this anisotropy is induced by the initial condition, which propagates in the z -direction. Thus, it is only because of the initial condition that the dynamics in z occurs on a different length-scale than in x and y .

2.12 The Dimensionless Linear Schrödinger Equation

2.12.1 Paraxial Approximation

In Sect. 1.3 we derived the linear Schrödinger equation by applying the paraxial approximation to the scalar Helmholtz equation. The justification given there for the paraxial approximation was that solutions that propagate in the z -direction are “mainly” composed of paraxial plane waves. We now utilize the understanding that the characteristic length-scale for changes in z is given by the diffraction length (Sect. 2.11), to provide a different informal justification for the paraxial approximation.

Our starting point is the dimensional scalar Helmholtz equation

$$\Delta E(x, y, z) + k_0^2 E = 0.$$

Substituting $E = \psi(x, y, z)e^{ik_0 z}$ gives

$$\psi_{zz}(z, x, y) + 2ik_0 \psi_z + \psi_{xx} + \psi_{yy} = 0, \quad (2.60)$$

which is the Helmholtz equation in terms of ψ . In Sect. 2.11 we saw that the scaling of the independent variables is

$$\tilde{x} = \frac{x}{r_0}, \quad \tilde{y} = \frac{y}{r_0}, \quad \tilde{z} = \frac{z}{2L_{\text{diff}}}, \quad (2.61)$$

where r_0 is the input beam width, and $L_{\text{diff}} = r_0^2 k_0$ is the diffraction length. Substituting (2.61) in (2.60) and multiplying by r_0^2 gives the dimensionless Helmholtz equation

²⁸ See Sects. 1.7 and 2.12.

$$\frac{f^2}{4} \psi_{\tilde{z}\tilde{z}}(\tilde{z}, \tilde{x}, \tilde{y}) + i \psi_{\tilde{z}} + \psi_{\tilde{x}\tilde{x}} + \psi_{\tilde{y}\tilde{y}} = 0, \quad (2.62)$$

where f is given by (2.59).

Typically f^2 is very small (Observation 1.2). Therefore,²⁹

$$f^2 \psi_{\tilde{z}\tilde{z}} \ll \psi_{\tilde{z}}.$$

This suggests that we can apply the *paraxial approximation* and neglect $\psi_{\tilde{z}\tilde{z}}$, i.e., approximate (2.62) by the dimensionless Schrödinger equation

$$i \psi_{\tilde{z}}(\tilde{z}, \tilde{x}, \tilde{y}) + \psi_{\tilde{x}\tilde{x}} + \psi_{\tilde{y}\tilde{y}} = 0. \quad (2.63)$$

Conclusion 2.11 *The paraxial approximation amounts to neglecting $O(f^2)$ terms in the Helmholtz equation.*

Since the relative magnitude of nonparaxial effects is $O(f^2)$, f is called the *nonparaxiality parameter*.

Remark The parameter f also represents the ratio of the length-scale of the transverse and longitudinal coordinates, i.e.,

$$\frac{[x]}{[z]} = \frac{[y]}{[z]} = O(f), \quad (2.64)$$

see Sect. 2.11.

2.12.2 Focused Beams

In Conclusion 2.6 we saw that a lens located at $z = 0$ with a focal point at $(0, 0, F)$ is represented by the quadratic phase term $e^{-i \frac{k_0(x^2+y^2)}{2F}}$. To derive the corresponding expression for the dimensionless Schrödinger equation (2.63), we change to the dimensionless variables (2.61) and $\tilde{F} = \frac{F}{2L_{\text{diff}}}$. This gives

Conclusion 2.12 *In the dimensionless Schrödinger equation (2.63), the effect of a lens located at $\tilde{z} = 0$, whose focal point is at $(0, 0, \tilde{F})$, is represented by adding a quadratic phase term to the initial condition as follows:*

$$\underbrace{\tilde{\psi}_0(\tilde{x}, \tilde{y})}_{\text{no lens}} \rightarrow \underbrace{\tilde{\psi}_0(\tilde{x}, \tilde{y}) e^{-i \frac{\tilde{x}^2 + \tilde{y}^2}{4\tilde{F}}}}_{\text{with lens}}. \quad (2.65)$$

²⁹ This is the dimensionless analog of $\psi_{zz} \ll k_0 \psi_z$.

Remark Since the dimensional and dimensionless Schrödinger equations are $2ik_0\psi_z + \Delta_\perp\psi = 0$ and $i\psi_z + \Delta_\perp\psi = 0$, respectively, one can obtain the dimensionless expression of the phase by “substituting $k_0 = 1/2$ ” in the dimensional expression.

Exercise 2.12 Verify that $\tilde{F} = O(1) \iff \frac{r_0}{\tilde{F}} = O(f)$. Conclude that if the rescaled focal distance is $O(1)$, the (dimensional) input beam is paraxial.

2.12.3 Tilted Beams

In Conclusion 2.7 we saw that in the dimensional Schrödinger model, a tilt in the direction of the unit vector $\mathbf{n} = (n_x, n_y, n_z)$ is represented by the linear phase term $e^{i\frac{k_0}{n_z}(n_x x + n_y y)}$. To derive the corresponding dimensionless expression, we change to the dimensionless variables (2.61). This yields

$$e^{i\frac{k_0}{n_z}(n_x x + n_y y)} = e^{i\frac{k_0}{n_z}r_0(n_x \tilde{x} + n_y \tilde{y})} = e^{i\frac{c_x \tilde{x} + c_y \tilde{y}}{2}}, \quad (c_x, c_y) = \frac{2r_0 k_0}{n_z}(n_x, n_y).$$

Since the scaling of x and y is different from that of z , the direction of the tilted beam in the dimensionless coordinates is

$$\left(\frac{n_x}{r_0}, \frac{n_y}{r_0}, \frac{n_z}{2L_{\text{diff}}} \right) = \frac{n_z}{2L_{\text{diff}}}(c_x, c_y, 1),$$

i.e., it points in the direction of $(c_x, c_y, 1)$.

Conclusion 2.13 In the dimensionless Schrödinger model (2.63), a tilt of the incoming beam in the direction of the vector $(c_x, c_y, 1)$ is represented by adding a linear phase term to the initial condition as follows:

$$\underbrace{\tilde{\psi}_0(\tilde{x}, \tilde{y})}_{\text{no tilt}} \rightarrow \underbrace{\tilde{\psi}_0(\tilde{x}, \tilde{y})e^{i\frac{c_x \tilde{x} + c_y \tilde{y}}{2}}}_{\text{with tilt}}.$$

Remark The dimensionless tilt angle $\tilde{\theta}$ is given by $\tan \tilde{\theta} = \frac{|\mathbf{c}|}{1} = |\mathbf{c}|$, where $\mathbf{c} = (c_x, c_y)$.

Exercise 2.13 Verify that $\mathbf{c} = O(1) \iff \frac{|\mathbf{n}_\perp|}{|n_z|} = O(f)$, where $\mathbf{n}_\perp = (n_x, n_y)$. Therefore, if the rescaled tilt angle $\tilde{\theta} = \arctan |\mathbf{c}|$ is $O(1)$, the dimensional tilt angle $\theta = \arctan \frac{|\mathbf{n}_\perp|}{|n_z|}$ is $O(f)$, and so the (dimensional) tilted beam is paraxial.

Exercise 2.14 Verify that if the dimensional tilted beam is paraxial, then

$$n_z = 1 + O(f^2). \quad (2.66)$$

Remark In Sect. 8.2 we will re-derive Conclusion 2.13 by using the (exact) Galilean invariance of the Schrödinger equation. This will show that the result of Conclusion 2.13 is exact, which is why in Sect. 2.8.5 we divided the phase by n_z .

2.12.4 Linear Schrödinger Equation in d Dimensions

In what follows, we drop the tilde signs and consider the dimensionless linear Schrödinger equation in d transverse dimensions

$$i\psi_z(z, \mathbf{x}) + \Delta_\perp \psi = 0, \quad \psi(0, \mathbf{x}) = \psi_0(\mathbf{x}), \quad (2.67)$$

where

$$\mathbf{x} = (x_1, \dots, x_d) \in \mathbb{R}^d, \quad \Delta_\perp = \frac{\partial^2}{\partial x_1^2} + \dots + \frac{\partial^2}{\partial x_d^2}.$$

The physical case of propagation of laser beams in a bulk medium is $d = 2$. Other dimensions, however, are also of physical interest. For example, $d = 1$ corresponds to propagation of laser beams in a planar waveguide, and $d = 3$ to propagation of laser pulses in a bulk medium in the anomalous dispersion regime (Sect. 4.1). The cases $d = 1, 2, 3$ are also of physical interest in quantum mechanics, where linear Schrödinger equation describes the temporal evolution of the quantum state of physical systems. In addition, in the nonlinear case, the cases $d = 1, 2, 3$ are of physical interest in the context of Bose-Einstein condensates (Sect. 4.2).

2.12.5 Generic Input Beams

We now extend the results of Sects. 2.12.2 and 2.12.3 to the d -dimensional linear Schrödinger equation (2.67).

- A real initial condition corresponds to a collimated input beam that propagates in the z -direction.
- A focused input beam that propagates in the z -direction is represented by

$$\psi_0(\mathbf{x}) = A_0(\mathbf{x})e^{-i\frac{|\mathbf{x}|^2}{4F}}, \quad (2.68)$$

where $A_0(\mathbf{x}) = |\psi_0(\mathbf{x})|$ is the beam amplitude, and F is the focal length.

- A tilted focused input beam that propagates in the (\mathbf{x}, z) -space in the direction of the vector $(\mathbf{c}, 1) \in \mathbb{R}^{d+1}$, where $\mathbf{c} = (c_1, \dots, c_d)$, is represented by

$$\psi_0(\mathbf{x}) = A_0(\mathbf{x})e^{-i\frac{|\mathbf{x}|^2}{4F}}e^{i\frac{\mathbf{c}\cdot\mathbf{x}}{2}}. \quad (2.69)$$

2.13 Fourier Transform

Before we begin to analyze the linear Schrödinger equation, let us recall some facts about the Fourier transform. Let $f(\mathbf{x})$ be a function defined for $\mathbf{x} \in \mathbb{R}^d$. The d -dimensional *Fourier transform* of f is

$$\hat{f}(\mathbf{k}) = \mathcal{F}(f(\mathbf{x})) := \frac{1}{(2\pi)^{\frac{d}{2}}} \int_{\mathbb{R}^d} f(\mathbf{x}) e^{-i\mathbf{k} \cdot \mathbf{x}} d\mathbf{x}, \quad (2.70)$$

where $\mathbf{k} = (k_1, \dots, k_d)$. The *inverse Fourier transform* is

$$f(\mathbf{x}) = \mathcal{F}^{-1}(\hat{f}(\mathbf{k})) := \frac{1}{(2\pi)^{\frac{d}{2}}} \int_{\mathbb{R}^d} \hat{f}(\mathbf{k}) e^{i\mathbf{k} \cdot \mathbf{x}} d\mathbf{k}.$$

The inverse Fourier transform of a product is a convolution, i.e.,

$$\mathcal{F}^{-1}(\hat{f}(\mathbf{k})\hat{g}(\mathbf{k})) = f * g(\mathbf{x}), \quad (2.71)$$

where

$$(f * g)(\mathbf{x}) := \frac{1}{(2\pi)^{\frac{d}{2}}} \int_{\mathbb{R}^d} f(\mathbf{x} - \mathbf{y})g(\mathbf{y}) d\mathbf{y}.$$

The Fourier transform of a Gaussian is a Gaussian, i.e.,

$$\mathcal{F}\left(e^{-p|\mathbf{x}|^2/2}\right) = p^{-\frac{d}{2}} e^{-|\mathbf{k}|^2/2p}, \quad \operatorname{Re}(p) \geq 0. \quad (2.72)$$

Finally, *Parseval's relation* is

$$\int_{\mathbb{R}^d} |f(\mathbf{x})|^2 d\mathbf{x} = \int_{\mathbb{R}^d} |\hat{f}(\mathbf{k})|^2 d\mathbf{k}. \quad (2.73)$$

2.14 L^p , H^1 , and H^2 Norms

For the analysis of the linear Schrödinger equation, we will need the following definitions.

Definition 2.2 (L^p norm) *The L^p norm of a function $f(\mathbf{x})$ is*

$$\|f\|_p := \begin{cases} \left(\int_{\mathbb{R}^d} |f(\mathbf{x})|^p d\mathbf{x} \right)^{\frac{1}{p}}, & \text{if } 1 \leq p < \infty, \\ \sup_{\mathbf{x} \in \mathbb{R}^d} |f(\mathbf{x})|, & \text{if } p = \infty. \end{cases}$$

Definition 2.3 (H^1 norm) *The H^1 norm of $f(\mathbf{x})$ is*

$$\|f\|_{H^1} := \left(\|f\|_2^2 + \|\nabla_\perp f\|_2^2 \right)^{\frac{1}{2}} = \left(\int_{\mathbb{R}^d} |f(\mathbf{x})|^2 d\mathbf{x} + \int_{\mathbb{R}^d} |\nabla_\perp f(\mathbf{x})|^2 d\mathbf{x} \right)^{\frac{1}{2}},$$

where $\nabla_\perp = \left(\frac{\partial}{\partial x_1}, \dots, \frac{\partial}{\partial x_d} \right)$ and $|\nabla_\perp f|^2 = \left| \frac{\partial f}{\partial x_1} \right|^2 + \dots + \left| \frac{\partial f}{\partial x_d} \right|^2$.

Definition 2.4 (H^2 norm) *The H^2 norm of $f(\mathbf{x})$ is*

$$\|f\|_{H^2} := \left(\|f\|_2^2 + \|\nabla f\|_2^2 + \|\Delta f\|_2^2 \right)^{\frac{1}{2}}.$$

If $\|f\|_p < \infty$, we say that f is in L^p , and similarly for H^1 and H^2 .

2.15 Linear Schrödinger Equation—Analysis

In this section we analyze the linear Schrödinger equation (2.67).

2.15.1 Fundamental Solution

Lemma 2.9 *The solution of the linear Schrödinger equation (2.67) is*

$$\psi(z, \mathbf{x}) = \frac{1}{(4\pi iz)^{\frac{d}{2}}} \int e^{i \frac{|\mathbf{x}-\mathbf{y}|^2}{4z}} \psi_0(\mathbf{y}) d\mathbf{y}. \quad (2.74)$$

Proof Let $\hat{\psi}(z, \mathbf{k}) = \mathcal{F}(\psi(z, \mathbf{x}))$. Taking the Fourier transform of Eq. (2.67) gives

$$i(\hat{\psi})_z - |\mathbf{k}|^2 \hat{\psi} = 0, \quad \hat{\psi}(0, \mathbf{k}) = \hat{\psi}_0(\mathbf{k}).$$

The solution of this ODE is

$$\hat{\psi}(z, \mathbf{k}) = e^{-i|\mathbf{k}|^2 z} \hat{\psi}_0(\mathbf{k}). \quad (2.75)$$

Therefore, by (2.71),

$$\psi = \mathcal{F}^{-1} \left(e^{-i|\mathbf{k}|^2 z} \right) * \psi_0.$$

Substituting $p = 1/2iz$ in (2.72) gives

$$\mathcal{F}^{-1} \left(e^{-i|\mathbf{k}|^2 z} \right) = \frac{1}{(2iz)^{\frac{d}{2}}} e^{i \frac{|\mathbf{x}|^2}{4z}}. \quad (2.76)$$

Hence, the result follows. □

Remark A different explicit expression for the solution of (2.67) is given in Lemma 2.14.

If $\psi_0 = \delta(\mathbf{x})$, then $\psi = G$, where

$$G(z, \mathbf{x}) = \frac{1}{(4\pi iz)^{\frac{d}{2}}} e^{i \frac{|\mathbf{x}|^2}{4z}}. \quad (2.77)$$

Therefore, $G(z, \mathbf{x})$ is the fundamental solution of the linear Schrödinger equation (2.67):

Lemma 2.10 *Let G be given by (2.77). Then*

$$iG_z(z, \mathbf{x}) + \Delta_{\perp} G = 0, \quad z > 0, \quad \mathbf{x} \in \mathbb{R}^d,$$

and $\lim_{z \rightarrow 0+} G(z, \mathbf{x}) = \delta(\mathbf{x})$.

The result of Lemma 2.9 can also be rewritten as

Corollary 2.5 *The solution of the linear Schrödinger equation (2.67) is*

$$\psi(z, \mathbf{x}) = (2\pi)^{\frac{d}{2}} G * \psi_0. \quad (2.78)$$

Exercise 2.15 *Prove Lemmas 2.9 and 2.10 directly, by using the definition of G and the relation $\int_{-\infty}^{\infty} e^{is^2} ds = e^{i\pi/4} \sqrt{\pi}$.*

Remark A “careless derivation” of the fundamental solution of the Schrödinger equation is as follows. If we formally make the change of variables $z = -it$, then (2.67) becomes the heat equation $\psi_t(t, \mathbf{x}) = \Delta_{\perp} \psi$. It is well known that the fundamental solution of the heat equation is $G(t, \mathbf{x}) = (4\pi t)^{-\frac{d}{2}} e^{-\frac{|\mathbf{x}|^2}{4t}}$. If we change back from t to z , we “get” that the fundamental solution of the Schrödinger equation is given by (2.77). There is, however, a fundamental difference between these two kernels: The heat kernel is exponentially decaying, hence it is highly regularizing. In contrast, the Schrödinger kernel is oscillatory. Hence, it is only mildly regularizing.

2.15.2 Existence and Smoothness

In Sect. 2.10 we saw that in linear paraxial propagation³⁰ of focused Gaussian input beams, collapse occurs under the geometrical optics approximation, but not if diffraction is not neglected. More generally, one can prove that diffraction prevents singularities in linear optics, by showing that all solutions of the linear Schrödinger equation exist and are bounded for $0 \leq z < \infty$.

³⁰ I.e., in the linear Schrödinger model.

In general, existence and smoothness of solutions of the linear Schrödinger equation (2.67) depend on properties of their initial condition. When ψ_0 corresponds to an input laser beam, we can assume that it is bounded and that it decays sufficiently fast as $|\mathbf{x}| \rightarrow \infty$. In what follows, we present some rigorous results that show that under these conditions, the solution of (2.67) exists for all $z \geq 0$. This implies, in particular, that a focusing lens does not lead to a singularity if one applies the paraxial approximation (i.e., uses the Schrödinger model instead of the Helmholtz model), but does not apply the geometrical optics approximation (i.e., does not neglect diffraction). Therefore, we have

Conclusion 2.14 *Diffraction arrests collapse in linear paraxial propagation.*

Let us begin with the case where $\psi_0 \in L^1$, i.e., $\int_{\mathbb{R}^d} |\psi_0| d\mathbf{x} < \infty$.³¹ By (2.74),

$$\sup_{\mathbf{x} \in \mathbb{R}^d} |\psi(\mathbf{x}, z)| \leq (4\pi z)^{-\frac{d}{2}} \int_{\mathbb{R}^d} |\psi_0| d\mathbf{x}, \quad z > 0.$$

Therefore, the solution of (2.67) is bounded for all $\mathbf{x} \in \mathbb{R}^d$ and $z > 0$. In particular, diffraction prevents the amplitude $|\psi|$ from becoming infinite. Moreover, if $\psi_0 \in L^1$ and has a compact support, then ψ is analytic, since differentiation under the integral sign in (2.74) is justified.

“Unfortunately”, the L^1 norm does not have a physical meaning in optics. Rather, the physical condition that the input beam has a finite power is $\psi_0 \in L^2$, i.e., $\int_{\mathbb{R}^d} |\psi_0|^2 d\mathbf{x} < \infty$. In that case, the following holds:

Lemma 2.11 (conservation of L^2 norm) *Let ψ be a solution of linear Schrödinger equation (2.67), such that $\psi_0 \in L^2(\mathbb{R}^d)$. Then*

$$\|\psi\|_2^2 \equiv \|\psi_0\|_2^2, \quad z > 0,$$

where $\|\psi\|_2^2 := \int_{\mathbb{R}^d} |\psi|^2 d\mathbf{x}$.

Proof By (2.75), $|\hat{\psi}(z, \mathbf{k})| = |\hat{\psi}_0(\mathbf{k})|$. Therefore,

$$\int_{\mathbb{R}^d} |\psi(z, \mathbf{x})|^2 d\mathbf{x} = \int_{\mathbb{R}^d} |\hat{\psi}(z, \mathbf{k})|^2 d\mathbf{k} = \int_{\mathbb{R}^d} |\hat{\psi}_0|^2 d\mathbf{k} = \int_{\mathbb{R}^d} |\psi_0(\mathbf{x})|^2 d\mathbf{x},$$

where in the first and last equalities we used Parseval’s relation (2.73). □

Remark See Lemma 5.1 for a different proof of this result.

Remark Lemma 2.11 implies that *the power of a laser beam is conserved* in linear paraxial propagation.

³¹ See Sect. 2.14 for definitions of L^p and H^1 norms and spaces.

The NLS theory presented in this book is mostly in H^1 , i.e., for solutions $\psi(z, \mathbf{x})$ such that $\psi(z) \in H^1(\mathbb{R}^d)$, see Sect. 5.5. In particular, an NLS solution becomes singular if and only if its H^1 norm becomes infinite (Corollary 5.3). We now show that in the linear case, the H^1 norm of ψ is conserved:

Corollary 2.6 (conservation of H^1 norm) *Let ψ be a solution of linear Schrödinger equation (2.67), such that $\psi_0 \in H^1$. Then*

$$\|\psi\|_{H^1} \equiv \|\psi_0\|_{H^1}, \quad z > 0,$$

where $\|\psi\|_{H^1}^2 := \int_{\mathbb{R}^d} (|\psi|^2 + |\nabla_{\perp} \psi|^2) d\mathbf{x}$ and $|\nabla_{\perp} \psi|^2 = \sum_{k=1}^d |\frac{\partial \psi}{\partial x_k}|^2$.

Exercise 2.16 *Prove Corollary 2.6.*

Thus, when $\psi_0 \in H^1$, the H^1 norm of the solution ψ of the linear Schrödinger equation does not become infinite. If, in addition, ψ_0 decays sufficiently fast as $|\mathbf{x}| \rightarrow \infty$, then ψ is smooth, since differentiation under the integral sign in (2.74) is justified.

For comprehensive surveys of rigorous results on existence and smoothness of solutions of the linear Schrödinger equation, see e.g., [249, Sect. 3.1] and [39, Chap. 2].

2.15.3 Gaussian Beams

From expression (2.78) follows

Lemma 2.12 *Any solution of the linear Schrödinger equation (2.67) with a Gaussian initial condition maintains a Gaussian profile for all $z > 0$.*

Proof Since the Fourier transform of a Gaussian is a Gaussian, see (2.72), and the product of two Gaussians is a Gaussian, it follows that $\hat{\psi} = e^{-i|\mathbf{k}|^2 z} \hat{\psi}_0$ is a Gaussian. Hence, by (2.72), so is ψ . \square

Lemma 2.12 explains why the Gaussian ansatz (2.49) leads to an exact solution of the linear Schrödinger equation, and also why this aberrationless property is unique to Gaussian profiles in linear propagation. In Sect. 3.5 we shall see that the Gaussian ansatz was also used in nonlinear propagation. In that case, however, it is an *approximation*.

Expression (2.78) enables us to explicitly solve the linear Schrödinger equation with a Gaussian initial condition:

Lemma 2.13 *The solution of the linear Schrödinger equation (2.67) with $\psi_0(\mathbf{x}) = e^{-|\mathbf{x}|^2}$ is*

$$\psi(z, \mathbf{x}) = \frac{1}{(1 + 4iz)^{\frac{d}{2}}} e^{-\frac{|\mathbf{x}|^2}{1 + 4iz}}. \quad (2.79)$$

Proof Let us first recall that if $G_\sigma(\mathbf{x}) = \left(\frac{1}{2\pi\sigma}\right)^{\frac{d}{2}} e^{-\frac{|\mathbf{x}|^2}{2\sigma}}$, then

$$G_{\sigma_1} * G_{\sigma_2} = \left(\frac{1}{2\pi}\right)^{\frac{d}{2}} G_{\sigma_1 + \sigma_2}. \quad (2.80)$$

Indeed, (2.72) implies that $\widehat{G_\sigma} = \left(\frac{1}{2\pi}\right)^{\frac{d}{2}} e^{-\frac{\sigma|\mathbf{k}|^2}{2}}$. Therefore,

$$\widehat{G_{\sigma_1} * G_{\sigma_2}} = \left(\frac{1}{2\pi}\right)^d \widehat{G_{\sigma_1 + \sigma_2}}.$$

Transforming back and using (2.71) gives (2.80).

Returning to the solution of the linear Schrödinger equation, let us note that $\psi_0 = e^{-|\mathbf{x}|^2} = \pi^{\frac{d}{2}} G_{\sigma=\frac{1}{2}}$, and the Schrödinger kernel (2.77) is equal to $G_{\sigma=2iz}$. By relations (2.78) and (2.80),

$$\psi = (2\pi)^{\frac{d}{2}} G * \psi_0 = (2\pi)^{\frac{d}{2}} G_{2iz} * \pi^{\frac{d}{2}} G_{\frac{1}{2}} = \pi^{\frac{d}{2}} G_{2iz + \frac{1}{2}}.$$

Therefore, we proved (2.79). \square

Remark Expression (2.79) is useful, among other things, for testing the linear part of numerical solvers of the NLS (Sect. 29.5).

We can rewrite (2.79) as

$$\psi(z, \mathbf{x}) = \frac{1}{(1 + 4iz)^{\frac{d}{2}}} e^{-\frac{1-4iz}{1+16z^2} |\mathbf{x}|^2}.$$

Since

$$|\psi| = \frac{1}{L^{\frac{d}{2}}(z)} e^{-\frac{|\mathbf{x}|^2}{L^2(z)}}, \quad L(z) = \sqrt{1 + 16z^2},$$

it follows that ψ has a self-similar Gaussian profile, whose width and amplitude are proportional to $L(z)$ and $L^{-\frac{d}{2}}(z)$, respectively. In addition, since

$$\arg \psi(z, \mathbf{x}) = \arg \psi(z, 0) + \frac{4z|\mathbf{x}|^2}{1 + 16z^2},$$

where

$$\arg \psi(z, 0) = \arg \frac{1}{(1 + 4iz)^{\frac{d}{2}}} = -\frac{d}{2} \arctan(4z),$$

the real and imaginary parts of ψ develop spatial oscillations, which become ever faster as $|\mathbf{x}| \rightarrow \infty$.

2.15.4 Dispersive Equation

To understand why the Gaussian beam (2.79) develops spatial oscillations, let us first note that $\psi = e^{-i\omega z + i\mathbf{k} \cdot \mathbf{x}}$ is a linear mode of the Schrödinger equation (2.67), provided that ω and \mathbf{k} satisfy the dispersion relation $\omega = |\mathbf{k}|^2$. Therefore, we can explicitly write the solution of the linear Schrödinger equation as follows:

Lemma 2.14 *The solution of the linear Schrödinger equation (2.67) is*

$$\psi(z, \mathbf{x}) = \frac{1}{(2\pi)^{\frac{d}{2}}} \int \hat{\psi}_0(\mathbf{k}) e^{-i\omega(\mathbf{k})z + i\mathbf{k} \cdot \mathbf{x}} d\mathbf{k}, \quad \omega(\mathbf{k}) = |\mathbf{k}|^2. \quad (2.81)$$

The linear modes can be written as

$$e^{-i\omega(\mathbf{k})z + i\mathbf{k} \cdot \mathbf{x}} = e^{-i|\mathbf{k}|(v_{\text{phase}}z - \frac{\mathbf{k}}{|\mathbf{k}|} \cdot \mathbf{x})}, \quad v_{\text{phase}} := \frac{\omega(\mathbf{k})}{|\mathbf{k}|} = |\mathbf{k}|.$$

Since each wavenumber travels at a different phase velocity, “any” solution of the linear Schrödinger equation (and not only Gaussian beams) “disintegrates” and develops spatial oscillations as it propagates.

Exercise 2.17 *Explain why the spatial oscillations become faster as $|\mathbf{x}| \rightarrow \infty$.*

The term *dispersive* is misleading in the context of the Schrödinger equation in optics. Indeed, physical dispersion refers to the situation where different temporal frequencies propagate at different phase velocities $v_{\text{phase}} = c/n_0(\omega)$, see Sect. 35.1.1. Since the Schrödinger equation models the propagation of a single temporal frequency, there is no “physical dispersion” in this model. The “dispersion” in the Schrödinger model should thus be viewed as “mathematical dispersion”, i.e., it has the mathematical properties of physical dispersion. This is analogous (and related) to viewing the variable z in the Schrödinger equation in optics as a “time-like” variable, although z has nothing to do with physical time.³²

2.16 Non-directionality (Reversibility)

In most of this book we will consider the nonlinear Schrödinger equation

$$i\psi_z(z, \mathbf{x}) + \Delta\psi + |\psi|^{2\sigma}\psi = 0, \quad z > 0, \quad \psi(0, \mathbf{x}) = \psi_0(\mathbf{x}). \quad (2.82)$$

³² The dispersive character of the Schrödinger equation in optics is not due to the paraxial approximation, since the linear Helmholtz equation is also “mathematically dispersive”. Indeed, the dispersion relation for the linear modes $E = e^{-i\omega z + i\mathbf{k} \cdot \mathbf{x}}$ of the Helmholtz equation (2.22) is $\omega = \sqrt{k_0^2 - |\mathbf{k}|^2}$, and so $\omega/|\mathbf{k}| \neq \text{constant}$. This dispersion is also mathematical and not optical, since the Helmholtz equation models the propagation of a single temporal frequency.

Both the linear and the nonlinear Schrödinger equation are considered as initial value problems, solved for increasing values of z . Any result for these equations can be applied, however, to the Schrödinger equation with decreasing values of z . This follows from the fact that the Schrödinger equation is invariant under the *reversibility transformation*³³

$$z \rightarrow -z \quad \text{and} \quad \psi \rightarrow \psi^*.$$

Lemma 2.15 *Let $\psi(z, \mathbf{x})$ is a solution of the linear or nonlinear Schrödinger equation with initial condition $\psi_0(\mathbf{x})$. Then $\psi^*(-z, \mathbf{x})$ is a solution of the Schrödinger equation with initial condition $\psi_0^*(\mathbf{x})$.*

In particular, since ψ becomes singular if and only if ψ^* does so, as far as collapse is concerned, it “does not matter” whether the equation is for ψ or for ψ^* .

The reversibility in z of the Schrödinger equation sets it apart from the heat equation $iu_t(t, \mathbf{x}) = \Delta u$, which is well-posed for increasing values of t , but ill-posed for decreasing values of t . In the case of the heat equation, this directionality reflects the difference between moving forward and backward in time. In contrast, in the Schrödinger model, there is no physical difference between increasing z (moving to the right) and decreasing z (moving to the left).

2.16.1 Symmetry with Respect to z_{\min}

The width of a focused Gaussian beam is, see (2.57),

$$L^2(z) = \left(\frac{1}{F^2} + \frac{1}{L_{\text{diff}}^2} \right) (z - z_{\min})^2 + L_{\min}^2,$$

where z_{\min} is the location of the minimal width L_{\min} . Therefore,

$$L(z_{\min} - z) = L(z_{\min} + z),$$

i.e., $L(z)$ is symmetric with respect to z_{\min} . Indeed, because of the non-directionality in z , for any beam collimated at z_{\min} ,³⁴ the propagation dynamics to the right of z_{\min} is the same as that to the left of z_{\min} :

Lemma 2.16 *Let ψ be a solution of the linear or nonlinear Schrödinger equation which is collimated at z_{\min} , i.e.,*

$$\psi(z_{\min}, \mathbf{x}) = e^{i\alpha} f(\mathbf{x}), \quad \text{where } \alpha \text{ and } f(\mathbf{x}) \text{ are real.} \quad (2.83)$$

³³ This reversibility property also holds for the rays of the eikonal equation (Lemma 2.2).

³⁴ To see that the Gaussian beam is collimated at z_{\min} , note that by (2.49), it can be written as $\psi = A(z, \mathbf{x}) e^{i \frac{L_z(z)}{L} \frac{|\mathbf{x}|^2}{2} + i \zeta(z)}$, where A is real. Since $L(z)$ attains its minimum at z_{\min} , then $L_z(z_{\min}) = 0$, and so (2.83) holds. Intuitively, the Gaussian beam is collimated at z_{\min} , since it is focusing for $z < z_{\min}$ and defocusing for $z > z_{\min}$.

Then

$$\psi(z_{\min} + z, \mathbf{x}) = e^{2i\alpha} \psi^*(z_{\min} - z, \mathbf{x}).$$

In particular,

$$|\psi(z_{\min} + z, \mathbf{x})| = |\psi(z_{\min} - z, \mathbf{x})|.$$

Proof Let $\psi_{-\alpha} := e^{-i\alpha} \psi$. Then $\psi_{-\alpha}$ is a solution of the Schrödinger equation that satisfies $\psi_{-\alpha}(z_{\min}, \mathbf{x}) = f(\mathbf{x})$, where $f(\mathbf{x})$ is real. Therefore, by Lemma 2.15, $\psi_{-\alpha}(z_{\min} + z, \mathbf{x}) = \psi_{-\alpha}^*(z_{\min} - z, \mathbf{x})$. Hence, the result follows. \square

Remark In Lemma 38.4 we will use this result to characterize the continuations of singular NLS solutions which are symmetric with respect to the singularity point Z_c .

2.16.2 Sign of Diffraction (and Nonlinearity)

Let $\psi(z, \mathbf{x})$ be a solution of the linear Schrödinger equation

$$i\psi_z(z, \mathbf{x}) + \Delta\psi = 0, \quad z > 0, \quad \psi(0, \mathbf{x}) = \psi_0(\mathbf{x}),$$

where ψ_0 is real. Then, $\psi^*(z, \mathbf{x})$ is a solution of the Schrödinger equation with the opposite sign of diffraction but the same initial condition

$$i\psi_z^*(z, \mathbf{x}) - \Delta\psi^* = 0, \quad z > 0, \quad \psi^*(0, \mathbf{x}) = \psi_0(\mathbf{x}).$$

Since $|\psi| = |\psi^*|$, we conclude that, by itself, the sign of the diffraction term does not affect the dynamics of $|\psi|$.

The above conclusion also holds in the nonlinear case. Indeed, let ψ be a solution of the NLS (2.82), and let ψ_0 be a real function. Then ψ^* is a solution of

$$i\psi_z^*(z, \mathbf{x}) - \Delta\psi^* - |\psi^*|^{2\sigma}\psi^* = 0, \quad z > 0, \quad \psi^*(0, \mathbf{x}) = \psi_0(\mathbf{x}),$$

i.e., of the NLS with the opposite signs of diffraction and nonlinearity but the same initial condition. Since $|\psi| = |\psi^*|$, the sign of nonlinearity by itself does not determine whether the nonlinearity is focusing or defocusing.³⁵

2.17 Singularities in Linear and Nonlinear Optics

In this chapter we saw that under the geometrical optics approximation, solutions of the Helmholtz and Schrödinger equations with initial conditions that correspond to a focused input beam, collapse at the focal point as a δ -function. If one does not

³⁵ Whether the nonlinearity is focusing or defocusing depends on the *relative signs* of nonlinearity and diffraction (Sect. 5.9).

make the geometrical optics approximation, however, these solutions do not shrink to a point.

Conclusion 2.15 *In linear propagation, focused initial conditions become singular if and only if we apply the geometrical optics approximation. In other words, diffraction arrests collapse in linear optics.*

In Sect. 3.4 we shall see that Conclusion 2.15 does not extend to the nonlinear case, i.e., diffraction does not always arrest collapse of NLS solutions.

Since solutions of the linear Schrödinger equation exist globally, we have

Conclusion 2.16 *In linear propagation, the paraxial approximation does not lead to a singularity.*

In Sect. 34.8 we shall see that there exist solutions of the scalar nonlinear Helmholtz equation that exist globally, for which the corresponding NLS solutions become singular. Therefore, Conclusion 2.16 does not extend to nonlinear propagation.

<http://www.springer.com/978-3-319-12747-7>

The Nonlinear Schrödinger Equation
Singular Solutions and Optical Collapse

Fibich, G.

2015, XXXI, 862 p. 202 illus., 100 illus. in color.,

Hardcover

ISBN: 978-3-319-12747-7